PHYSICAL HUMAN ROBOT INTERACTION USING MODEL REFERENCE NEUROADAPTIVE CONTROL

By

SHAIKH MD RUBAYIAT TOUSIF

Presented to the Faculty of the Graduate School of

The University of Texas at Arlington in Partial Fulfillment

of the Requirements

for the Degree of

MASTER OF SCIENCE IN ELECTRICAL ENGINEERING

THE UNIVERSITY OF TEXAS AT ARLINGTON

May 2014

Acknowledgements

I would like to thank Professor Dr. Frank Lewis for giving me an opportunity to work with him. His vast knowledge in the areas of control system has motivated me to design the Model Reference Neuroadaptive controller. I would also like to thank him for giving me time every week and discussing a subject matter in great details.

Some of the courses taught by Dr. Frank Lewis were instrumental in developing my knowledge in the field of control system. Courses like Optimal Control Theory, Distributed Controls and Intelligent Controls helped me hone my understanding in this area and have given me enough of a background to work in this field in future.

I would also like to thank PhD students Bakur Al-Quaidi and Isura Ranatunga for always providing with ideas and suggestions to make a problem more interesting and also for being such great co-authors.

The support received from the NSF grant is gratefully acknowledged.

.

April 18, 2014

Abstract

PHYSICAL HUMAN ROBOT INTERACTION USING MODEL REFERENCE NEUROADAPTIVE CONTROL

Shaikh Md. Rubayiat Tousif, MSc.

The University of Texas at Arlington, 2014

Supervising Professor: Frank. L. Lewis

In this work Physical Human-Robot Interaction (*pHRI*) related problems are addressed as a part of the research going on in Assistive Robotics in the University of Texas Research Institute (UTARI). A novel model reference Neuroadaptive controller is designed based on existing technology of Lewis et al.

Adaptive impedance control is an important method for force/motion control of robotic systems. Most of the work in adaptive impedance control makes the error dynamics of the system to look like a prescribed model. By contrast, this work does not want the error dynamics to be prescribed as an impedance model. It makes the robot itself feel like a prescribed impedance model. Model reference behavior is introduced which allows to control the interaction behavior by changing the parameters suitably in the model. The novel controller makes the nonlinear dynamics of the robot to look like a linear model which will be more convenient for humans to interact with during task manipulation.

In this thesis a new inner-outer loop Neuroadaptive controller is formulated that makes pHRI robust to changes in both co-robot and human user. First, an inner-loop controller with guaranteed robustness and stability causes a robot to behave like a

prescribed robot impedance model. Second, an outer-loop controller tunes the impedance model so that the robot system assists humans with varying levels of skill to achieve task-specific objectives.

The controller developed in this work has been proved to work and to facilitate the illustration of the theories established, extensive simulations have been carried out on a 2 DOF robotic arm. The simulations results show good agreements with the theoretical concepts.

Table of Contents

List of Illustrations

Chapter 1

Introduction

In order for robots to move into the real world, do what humans do, learn how a task should be done and moreover assist human in completing a task, complex milestones are yet to be reached in the field of robotics research. The intent of this work is to explore research problems regarding Physical Human-Robot Interaction (pHRI). The outcome of this research is expected to have broad applicability in areas of healthcare, home co-Robots, manufacturing, defense and everywhere humans and robots will co-exist.

A truly assistive robotic system could be taken as one where understanding and skills of the human operator will be enhanced as he/ she uses the robotic system. On top of that, while using the system the operator should not only learn how to use the system properly but also the system should assist the operator so that the combined performance of the human-robot system is acceptable and can overcome any harsh conditions that may arise in real time operation. In brief, an assistive system should be like a game played by two players (robot system and the operator) where each will interact with the other and knowledge about the game will be learnt by both and performance level of individual will be heightened.

pHRI related work is continuously being carried out by some of the research centers and it is also evident that impedance control is an important way of the force/motion control for any robotic systems. So, it will be worthwhile mentioning some of the notable works which fall in the vicinity of the pHRI and adaptive impedance control that has been used for better understanding and formulation of this work.

1.1 Literature Survey

In this section some of the works on human robot interaction and adaptive impedance control is discussed.

In [1] adaptive control and programming by demonstration have been used to teach a robot interact with a human in a two-way task needing distribution of the load between two partners. The robot adjusted its motion according to perceived forces after expecting the partner's intentions from a learned task model. Direct reproduction of the learned model may not always bring acceptable outcomes as humans represent a highly complex contact environment. So an adaptive impedance control algorithm was also proposed in addition to learning so as to compensate for the unmodeled uncertainties. The adaptive control scheme tuned the impedance parameters for precise reproduction of the task model.

Kalakrishnan et.al in [2] developed robots capable of fine manipulation skills. Reinforcement learning has been used in acquiring manipulation skills in compliant robots. Kinesthetic demonstration was used to initialize the initial position control policy for manipulation. The policy was augmented with a force/torque profile which was controlled in combination with the position trajectories. They used their own algorithm known as Policy Improvement and Path Integrals (PI^2) to learn the force/torque profiles by optimizing a cost function that measured task success.

In [3] reinforcement learning was used to learn complex motor skills for robotic manipulation for completing real world tasks. The method developed allowed to learn and acquire new motor skills starting from a mere demonstration. Predictive model of the task was learnt which allowed to learn proprioceptive sensor feedback to observer succeeding execution of task online and avoid actions when failure is predicted.

Suzuki et al. [4] designed a novel adaptive assistive control for a haptic interface system where they suggested that there must be an identifier to find the control characteristics of the user during operation and then the control input to the system must be adaptively tuned according to the identified user's control characteristics. Based on the previous method in [5] a truly adaptive variable impedance control for an assisting system was proposed. It specified that human learns the unknown dynamics of the machine and uses the identified model as an inverse model for the manipulation of the machine. They also gave the idea that if the operated machine's dynamics can be changed so as to be learned by the user, the performance of the overall system would be enhanced. So the original dynamics was replaced by a virtual impedance model in the loop. Thus, they showed successfully that adaptive impedance control techniques could be used to improve the human operator's performance in a point to point motion task.

Impedance control was originally proposed by Hogan [6] and is used to control the response of a system under the influence of external forces by prescribing a desired impedance behavior. [7, 8] discusses explicit force control using PI, PD and PID controllers with known system models. Lyapunov based control theory has been shown in [9] to control robotic system along with stability and robustness proofs. Identification of the object stiffness using force controller was discussed in [10]. Adaptive impedance control blended with computed torque method was investigated in [11]. In [12] the problem of position/force tracking for constrained robot was addressed from an impedance control point of view. Position tracking error was used to tune the desired impedance model. Neural network control method has been also used in adaptive impedance control [13]. In [14] parallel control scheme was shown which combined hybrid force/position control with impedance control.

1.2 Problem Statement

Impedance control can be broadly classified into two categories. One in which stiffness parameters of the environment are estimated [7, 8, 10, 11, 12]. Second, human robot interactive forces where impedances parameters of interaction are tuned [1, 2, 3, and 4]. In this work problem relating the second type is addressed. Also a trajectory following task is not wanted, rather a more general one so that the task is closed around the human and the robot. Also programming a trajectory following task into the robot is not the motive in this work.

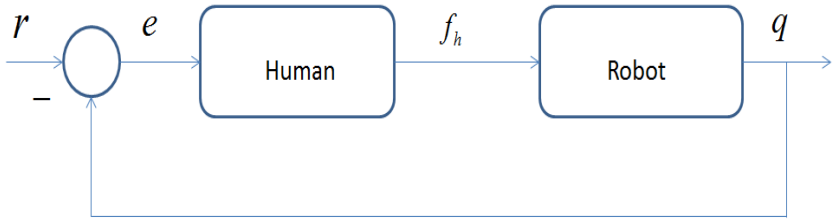

Figure 1: Human – Robot System

When humans interact with a robotic system it applies forces on it either in task or in Cartesian space, f_h as shown in figure 1. In this scenario the human applies forces and observes the robot dynamics q, and depending on these observations and the desired output r, the human will modify the forces being applied. The human acts like an outer loop force controller for the robotic system. Using Jacobian transpose these forces can be traced to joint torques. Conventional position controllers will see these human input torques as a disturbances τ_d and reject its effect. Interactions between humans and robotic system are generally complex and nonlinear. However, human learns a compensation model for the nonlinear dynamics and also a task specific controller. This

is a slow learning process and often requires high mental workload. Inspired by [4] the objective of this work is to use the operator's force f_h acting on the robotic system during interaction and also to make the whole system behave like a desired model, see figure 2.

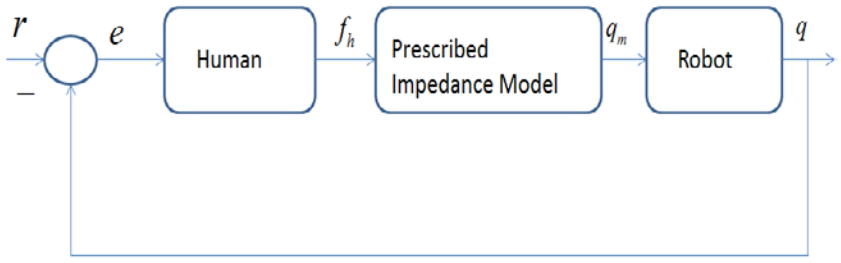

Figure 2: Human-Desired Model –Robot System

Under this circumstances none of the traditional error dynamics based force controller will be useful as those requires a reference trajectory, r but in reality only the forces exerted by the operator on the robotic system exists as input.

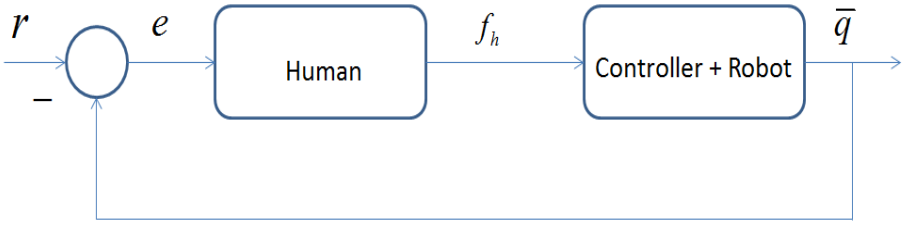

Figure 3: Human-–Robot Linearized System

This problem of how to use the operator's forces during interaction with the robotic system is addressed in this work. A novel Neuroadaptive controller has been developed that will make the robot system track a tunable desired model as shown in figure 3. The controller makes the robot and the controller combined look like a desired

model and the human will see this modified dynamics, $\overline{q}$. The human robot interaction behavior can be controlled by changing the model parameters for this kind of tunable controller. This novel way allows us to make the nonlinear dynamics of the robot to look like a linear model which will be more convenient for humans to interact with during task manipulation.

1.3 Contribution of this Work

A new neuroadaptive controller is formulated that differs from a standard trajectory following controllers by not requiring a desired trajectory. The task specific; trajectory following or otherwise are closed around a loop with human and the robots.

The closed loop error dynamics do not contain the prescribed model parameters. This makes it easier for the human to control or close the outer loop and use adaptive robotic interfaces.

The famous crossover model says that the transfer function of the human in a human in the loop system become accustomed so as to keep the complete system unchanged under the variation of the controlled system dynamics. This is achieved in the outer loop design.

1.4 Organization of this Thesis

In chapter 1 literature survey, the problem statement is provided. Chapter 2 discusses some application of Model Reference Adaptive Control and provides mathematical details of the Model Reference Neuro-adaptive Controller developed for this work. It provides necessary proofs and theorems. The effectiveness of the proposed controller and simulations carried out on a 2 DOF robotic arm are provided on chapter 3. In chapter 4 the outer loop design is provided. It puts the human in the loop and tries to

make the human and the robotic system respond like a desired model. Chapter 5 concludes the thesis and talks about future works that can be done to further this research.

Chapter 2

Model Reference Neuroadaptive Control

Model Reference Adaptive Control (MRAC) was originally proposed to solve problems were performance specifications are given in terms of a desired model. The desired model tells how the output of the process should respond ideally to a command input. The main approach developed in this work for tuning Human Robot Interface (HRI) is based on extending the technology invented by Lewis in the 1990s for neuroadaptive control of robot and nonlinear systems [15]. The contribution of this work is to provide a new reformulation of those methods by Lewis et al. to allow for the incorporation of model reference behavior in the robot interface. MRAC has been widely used in many control applications. Some of the works that used MRAC is given below.

In [16] optimized adaptive control and trajectory generation for a class of wheeled inverted pendulum models of vehicle system was investigated. The controlled vehicle dynamics was shaped so as to minimize motion tracking errors and angular accelerations. Adaptive control was developed using variable structure method to guarantee tracking of the reference model even in presence of external disturbances. The control objective was to make the closed loop dynamics of the controlled subsystem exactly match the dynamics of the reference model. The parameters of the reference model were chosen such that it guarantees motion tracking and also rider's comfort. Inspired by the real life scenario where human drivers manipulates the tilt angle to control the forward velocity a neural network based adaptive generator of implicit control trajectory of the tilt angle(AGICT) is designed. The AGICT indirectly controlled the forward velocity in such a way that the desired velocity was tracked asymptotically.

In [17] the problems relating the control of industrial robots with high speed continuous movements were examined using model reference adaptive control (MRACS)

method. The work proved that a manipulator belonging to a class converged to a suitable reference model using MRAS control.

Myoungho et al. [18] used MRAC technique for vehicle suspension system. Disturbances and vibrations were automatically reduced by tuning active suspension by MRAC. MRAC was designed using Lyapunov control theory and it could tolerate large changes in sprung load and suspension component characteristics and noticeable improvements over passive suspension was achieved.

In [19] MRAC was used to improve line power factor and lower line current harmonics for a single-phase shunt power filter. The MRAC was used over conventional proportional integral control due to its flexibility, adaptability, and robustness and especially its self-tuning ability of the gains to ensure system stability.

The subsequent sections of this chapter discuss in details about the controller formation and provide the mathematics and the necessary proofs.

2.1 Neuroadaptive Controller Formulation

In this section mathematical detail of new neuroadaptive controller that differs from a standard trajectory following controllers by not requiring a desired trajectory is provided. The task specific; trajectory following or otherwise are closed around a loop with human and the robots.

The dynamics of a robot system can be written as

$$M(\mathrm{q})\ddot{\mathrm{q}} + \mathrm{V}(\mathrm{q},\dot{\mathrm{q}})\dot{\mathrm{q}} + \mathrm{G}(\mathrm{q}) = \tau \qquad (1)$$

where $M(\mathrm{q})$ is the inertia matrix, $V(\mathrm{q},\dot{\mathrm{q}})$ is the Coriolis/centripetal vector, $G(\mathrm{q})$ is the gravity vector and q is the joint variable.

In reality, a robot arm is always affected by friction and disturbances. Therefore, it will be wise to add those terms in the robot dynamics to make it more generalized [20]. Therefore manipulator dynamics can be written as:

$$M(\mathrm{q})\ddot{\mathrm{q}} + \mathrm{V}(\mathrm{q},\dot{\mathrm{q}})\dot{\mathrm{q}} + F(\dot{\mathrm{q}}) + \mathrm{G}(\mathrm{q}) + \tau_d = \tau \qquad (2)$$

with $F(\dot{\mathrm{q}}) = F_v\dot{q} + F_d$, where F_v the coefficient matrix of viscous friction and F_d a dynamic friction term. Also added is a disturbance term τ_d , which could represent, for instance, any inaccurately modeled dynamics. Modeling friction is not easy and it may be the most contrary term to describe in the dynamics model. More on friction can be found in [21].

For this work the friction and disturbance terms are added to eq. (1) also the forces $f_h \in \Re^6$ in task space generated by human during interaction was added to it. So the general robot dynamics becomes:

$$M(\mathrm{q})\ddot{\mathrm{q}} + \mathrm{V}(\mathrm{q},\dot{\mathrm{q}})\dot{\mathrm{q}} + F(\dot{\mathrm{q}}) + \mathrm{G}(\mathrm{q}) + \tau_d = \tau + J^T f_h \qquad (3)$$

where J^T is the Jacobian transpose, $q \in \Re^n$, τ is the control torque.

Most of the robot control methods are special cases of ‘computed torque control’ according to Lewis et al. Computed torque control is a special application of feedback linearization of nonlinear systems. In this method, the nonlinearities of the system are cancelled by the method of feedback and thus techniques in linear control theory [22] can be applied.

A reference model whose dynamics will be followed by the robot is selected as

$$\bar{M}\ddot{q}_m + \bar{D}\dot{q}_m + \bar{K}q_m = J^T f_h \qquad (4)$$

where $\bar{M}$ is the mass matrix, D_m is the damping matrix, K_m is the spring constant matrix, and q_m is the model trajectory.

Note objective here is different than [7, 8, 10, 11, and 12] where the error dynamics are made to look like a prescribed model. In this formation there is no prescribed trajectory.

The error in the position was defined as

$$e = q_m - q \tag{5}$$

Differentiating eq. (5) twice with respect to time:

$$\dot{e} = \dot{q}_m - \dot{q} \quad or \quad \dot{q} = \dot{q}_m - \dot{e} \tag{6}$$

$$\ddot{e} = \ddot{q}_m - \ddot{q} \quad or \quad \ddot{q} = \ddot{q}_m - \ddot{e} \tag{7}$$

Filtered error is defined as:

$$r = \dot{e} + \Lambda_1 e + \Lambda_2 \varepsilon \tag{8}$$

Where, $\varepsilon = \int_0^t e(\tau) d\tau$

From eq. (8), eq. (9) can be written very easily.

$$\dot{e} = r - \Lambda_1 e - \Lambda_2 \varepsilon \tag{9}$$

Differentiating eq. (8) once with respect to time

$$\dot{r} = \ddot{e} + \Lambda_1 \dot{e} + \Lambda_2 e \tag{10}$$

From eq. (10), eq. (11) can be written very easily.

$$\ddot{e} = \dot{r} - \Lambda_1 \dot{e} - \Lambda_2 e \tag{11}$$

Therefore eq. (5) and eq. (7) can be written as

$$\dot{q} = \dot{q}_m - (r - \Lambda_1 e - \Lambda_2 \varepsilon) \tag{12}$$

$$\ddot{q} = \ddot{q}_m - (\dot{r} - \Lambda_1 \dot{e} - \Lambda_2 e) \tag{13}$$

respectively.

Substituting eq. (12) and eq. (13) in eq. (3)

$$M(\mathrm{q})(\ddot{q}_m - (\dot{r} - \Lambda_1 \dot{e} - \Lambda_2 e)) + V(\mathrm{q}, \dot{\mathrm{q}})(\dot{q}_m - (r - \Lambda_1 e - \Lambda_2 \varepsilon)) + F(\dot{\mathrm{q}}) + G(\mathrm{q}) + \tau_d = \tau + J^T f_h \tag{14}$$

$$M(\mathrm{q})\ddot{q}_m - M(\mathrm{q})\dot{r} + M(\mathrm{q})\Lambda_1 \dot{e} + M(\mathrm{q})\Lambda_2 e + V(\mathrm{q}, \dot{\mathrm{q}})\dot{q}_m - V(\mathrm{q}, \dot{\mathrm{q}})r + V(\mathrm{q}, \dot{\mathrm{q}})\Lambda_1 e + V(\mathrm{q}, \dot{\mathrm{q}})\Lambda_2 \varepsilon + F(\dot{\mathrm{q}}) + G(\mathrm{q}) + \tau_d = \tau + J^T f_h \tag{15}$$

$$-M(\mathrm{q})\dot{r} + M(\mathrm{q})(\ddot{q}_m + \Lambda_1 \dot{e} + \Lambda_2 e) - V(\mathrm{q}, \dot{\mathrm{q}})r + V(\mathrm{q}, \dot{\mathrm{q}})(\dot{q}_m + \Lambda_1 e + \Lambda_2 \varepsilon) + F(\dot{\mathrm{q}}) + G(\mathrm{q}) + \tau_d = \tau + J^T f_h \tag{16}$$

$$M(\mathrm{q})\dot{r} = M(\mathrm{q})(\ddot{q}_m + \Lambda_1 \dot{e} + \Lambda_2 e) - V(\mathrm{q}, \dot{\mathrm{q}})r + V(\mathrm{q}, \dot{\mathrm{q}})(\dot{q}_m + \Lambda_1 e + \Lambda_2 \varepsilon) + F(\dot{\mathrm{q}}) + G(\mathrm{q}) + \tau_d - \tau - J^T f_h \tag{17}$$

$$\therefore M(\mathrm{q})\dot{r} = -V(\mathrm{q}, \dot{\mathrm{q}})r + f(\mathrm{x}) + \tau_d - \tau - J^T f_h \tag{18}$$

where

$$f(\mathrm{x}) = M(\mathrm{q})(\ddot{q}_m + \Lambda_1 \dot{e} + \Lambda_2 e) + V(\mathrm{q}, \dot{\mathrm{q}})(\dot{q}_m + \Lambda_1 e + \Lambda_2 \varepsilon) + F(\dot{\mathrm{q}}) + G(\mathrm{q}) \tag{19}$$

Let the approximation based controller be

$$\tau = \hat{f} + K_v r - v(\mathrm{t}) - J^T f_h \tag{20}$$

Putting eq. (20) in eq. (18)

$$M(\mathrm{q})\dot{r} = -V(\mathrm{q}, \dot{\mathrm{q}})r + f(\mathrm{x}) + \tau_d - (\hat{f} + K_v r - v(\mathrm{t}) - J^T f_h) - J^T f_h \tag{21}$$

Simplifying the last equation the closed loop error dynamics is obtained.

$$\therefore M(\mathrm{q})\dot{r} = -V(\mathrm{q},\dot{\mathrm{q}})r - K_v r + \tilde{f} + \tau_d + v(\mathrm{t})$$

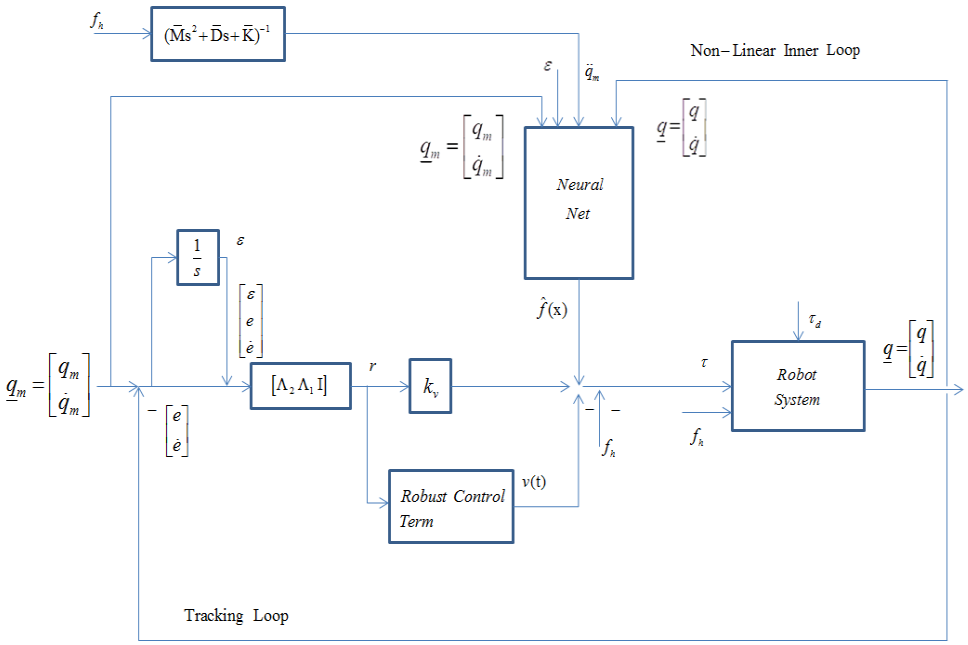

Figure 4: Model Reference Neuro-adaptive Control

Figure 4 shows the block diagram of the model reference neuro-adaptive control. It has a non-linear inner loop and a tracking loop.

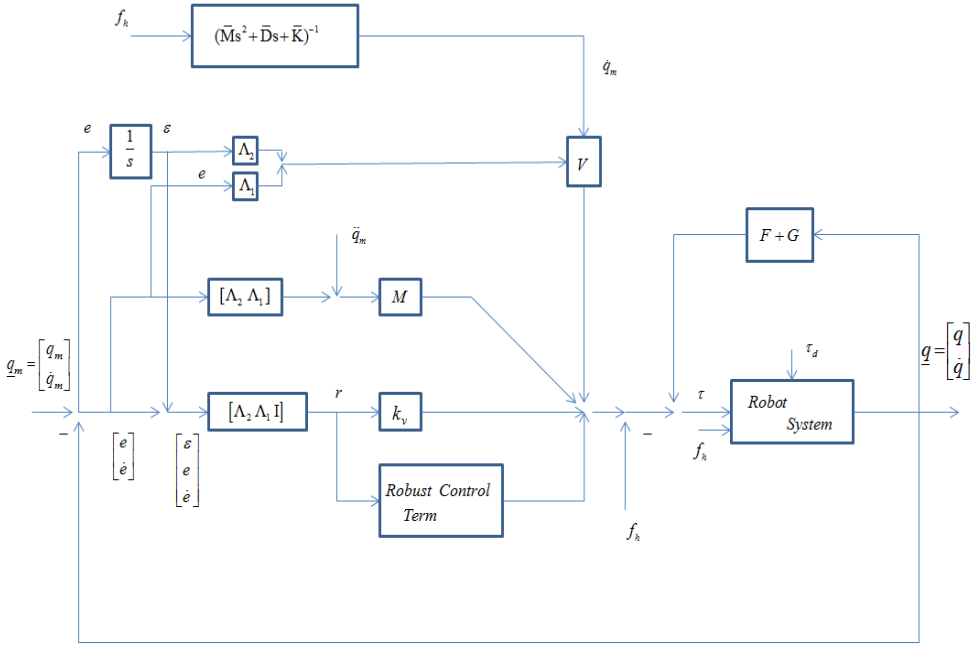

Figure 5: Model Reference Neuro-adaptive Control with breakdown

Figure 5 shows the MRNC without the neural network.

2.2 Inner Learning Loop Formulation

The learning loop performance and stability is based on previous work [23] [24]. Theorems and proofs for two cases are provided: a) Functional link neural network (FLNN) controller with augmented tuning to avoid persistence of excitation and b) Two-layer NN controller with augmented backprop tuning.

2.2.1 FLNN Controller with Augmented Tuning to Avoid PE

The unboundedness of the weight estimates when PE fails in adaptive control is known as ‘parameter drift’. The PE requirement in the following proof is to make sure that the drift does not occur. So σ modification is used to remedy this problem according to

[31]. Removing the PE condition results in a much more robust NN controller which is stable under wide variety of unmodeled dynamics and unforeseen situations. The controller is given below.

Control input:

$$\tau = \hat{W}^T \phi(\mathrm{x}) + \mathrm{K}_v r$$

NN Weight/ Threshold Tuning Algorithms:

$$\dot{\hat{W}} = F\phi(\mathrm{x})\,\mathrm{r}^T - kF \,\|\, \mathrm{r} \,\|\, \hat{\mathrm{W}}$$

Design parameter F is positive definite matrices, $k > 0$ a small design parameter.

Theorem 1: The ideal NN target weights are bounded by W_B , $\| W \|_F \leq W_B$. Let the control input for the robot arm be given by

$$\tau = \hat{W}^T \phi(\mathrm{x}) + \mathrm{K}_v r$$

With gain satisfying

$$K_{v_{\min}} > \frac{(\mathrm{k}\, W_B{}^2 / 4 + \varepsilon_N + d_B)(\mathrm{c}_0 + \mathrm{c}_2)}{b_x - q_B}.$$

Let the weight tuning be

$$\dot{\hat{W}} = F\phi r^T - kF \,\|\, r \,\|\, \hat{W}$$

With $F = F^T > 0$ and $k > 0$ a small design parameter. Making no assumptions on PE requirements on $\phi(\mathrm{x})$. Then the filtered tracking error $r(\mathrm{t})$ and the NN weight estimates $\hat{W}(\mathrm{t})$ are UUB with practical bounds given by (34) and (35). Moreover, the tracking error maybe made small as desired by increasing the tracking gain k_v .

Let the neural network approximation property given by equation 23 hold for the function $f(\mathrm{x})$ specified by equation 24 with a given accuracy ε_N for all x in the compact set $S_x \equiv \{x \mid \| x \| < b_x\}$ with $b_x > q_B$.

$$f(\mathrm{x}) = \mathrm{W}^T \phi(\mathrm{x}) + \varepsilon \tag{22}$$

$$f(\mathrm{x}) = M(\mathrm{q})(\ddot{q}_m + \Lambda_1 \dot{e} + \Lambda_2 e) + V(\mathrm{q}, \dot{\mathrm{q}})(\dot{q}_m + \Lambda_1 e + \Lambda_2 \varepsilon) + F(\dot{\mathrm{q}}) + G(\mathrm{q}) \tag{23}$$

$S_r \equiv \{r \mid \| r \| < (\mathrm{b}_x - \mathrm{q}_B)/(\mathrm{c}_0 + \mathrm{c}_2)\}$ is defined. Let $r(0) \in \mathrm{S}_r$. Then the approximation property holds.

A Lyapunov function candidate was selected according to equation 3.

$$L = \frac{1}{2} r^T M r + \frac{1}{2} tr\left\{\tilde{W}^T F^{-1} \tilde{W}\right\} \tag{24}$$

Differentiating equation 3 yields

$$\dot{L} = r^T M \dot{r} + \frac{1}{2} r^T \dot{M} r + tr\left\{\tilde{W}^T F^{-1} \dot{\tilde{W}}\right\} \tag{25}$$

Now substituting the closed loop filtered error dynamics in equation 4 yields

$$\dot{L} = -r^T K_v r + \frac{1}{2} r^T (\dot{\mathrm{M}} - 2\mathrm{V}_m) r + tr\left\{\tilde{W}^T (\mathrm{F}^{-1} \dot{\tilde{\mathrm{W}}} + \phi r^T)\right\} + r^T (\varepsilon + \tau_d) \tag{26}$$

Then using the tuning rule $\dot{\hat{W}} = F \phi r^T - kF \| r \| \hat{W}$ equation 5 becomes

$$\dot{L} = -r^T K_v r + K \| r \| tr\left\{\tilde{W}^T (W - \tilde{W})\right\} + r^T (\varepsilon + \tau_d) \tag{27}$$

Since

$$tr\left\{\tilde{W}^T (W - \tilde{W})\right\} = < W, \tilde{W} >_F - \| \tilde{W} \|^2_F \leq \| \tilde{W} \|_F \| W \|_F - \| \tilde{W} \|^2_F \tag{28}$$

With $\| . \|_F$ the Frobenius norm, there results

$$\dot{L} \leq \quad -K_{v_{\min}} \| r \|^2 + K \| r \| . \| \tilde{W} \|_F \, (W_B - \| \tilde{W} \|_F) + (\varepsilon_N + \mathrm{d}_B) \| r \| \tag{29}$$

$$= \quad - \| r \| \left[K_{v_{\min}} \| r \| + k \| \tilde{W} \|_F \, (\| \tilde{W} \|_F - W_B) - (\varepsilon_N + d_B) \right] \tag{30}$$

This is negative as long as the terms in braces are positive. Completing the square yields

$$K_{v_{\min}} \| r \| + K \| \tilde{W} \|_F \, (\| \tilde{W} \|_F - W_B) - (\varepsilon_N + d_B) \tag{31}$$

$$= \quad k(\| \tilde{W} \|_F - W_B / 2)^2 - k W_B^{\,2} / 4 + K_{v_{\min}} \| r \| - (\varepsilon_N + d_B) \tag{32}$$

Which is guaranteed positive as long as

$$\| r \| > \frac{k W_B^{\,2} / 4 + (\varepsilon_N + d_B)}{K_{v_{\min}}} \equiv b_r \tag{33}$$

Or

$$\| \tilde{W} \|_F > W_B / 2 + \sqrt{(\mathrm{k} W_B^{\,2} / 4 + (\varepsilon_N + d_B / \mathrm{k}))} \equiv b_W \tag{34}$$

Thus $\dot{L}$ is negative outside a compact set. Selecting the gain according to

$$K_{v_{\min}} > \frac{(\mathrm{k} W_B^{\,2} / 4 + \varepsilon_N + d_B)(\mathrm{c}_0 + \mathrm{c}_2)}{b_x - q_B} \tag{35}$$

ensures that the compact set defined by $\| r \| \leq b_r$ is contained in S_r, so that the approximation property holds throughout. This demonstrates the UUB of both $\| r \|$ and $\| \tilde{W}_B \|_F$.

At the error dynamics expression the terms r and $\tilde{W}^T$ are bonded by b_r and b_W respectively as shown above. V_m depends on $q, \dot{q}$ and as r is bounded q and $\dot{q}$ should be bounded as well. The only thing left is finding a bound on $\dot{r}$. Explicit bound is found on $\dot{r}$ is found from the error dynamics equation

$$\dot{r} = M^{-1} \left\{ -(\mathrm{K}_v + V_m) r + \tilde{W}^T \phi(\mathrm{x}) + (\varepsilon + \tau_d) + v \right\} \tag{36}$$

$$\| \dot{r} \| \leq \frac{1}{\sigma_{\min_{(M)}}} \left[(\sigma_{\max_{(K_v)}} + \sigma_{\max_{(Vm)}}) \| r \| + \sigma_{\max_{(W^T)}} \| \phi(x) \| + | \varepsilon | + | \tau_d | + | v | \right] \quad (37)$$

Equation number 38 gives an explicit bound on $\dot{r}$.

Details of the proof can be found in [15].

2.3 Two-Layer NN Controller with Augmented Backprop Tuning

Backprop tuning can only be guaranteed to work in an unrealistic ideal case. To meet the stability and tracking performance of a NN robot arm controller in the rough case that allows NN estimation errors and system disturbances modifications to the weight tuning rules and an addition of robustifying term $v(t)$ is required. Without these modifications it is impossible to show that the NN weights are bounded in general even though it is not difficult to show that $r(t)$ is bounded. The boundedness of the weights is needed to show that the control input $\tau(t)$ is bounded. In contrary to the ideal case, the tracking error is bounded by a small value rather than becoming zero. The controller is given below:

Control input:

$$\tau = \hat{W}^T \sigma(\hat{V}^T x) + K_v r - v$$

Robustifying Signal:

$$v(t) = -K_z(\| \hat{Z} \|_F + Z_B) r$$

NN Weight/ Threshold Tuning Algorithms:

$$\dot{\hat{W}} = F\hat{\sigma}r^T - F\hat{\sigma}'\hat{V}^T xr^T - kF \| \mathrm{r} \| \hat{\mathrm{W}}$$

$$\dot{\hat{V}} = Gx(\hat{\sigma}^{\mathrm{T}} \hat{\mathrm{W}}\mathrm{r})^T - kG \| \mathrm{r} \| \hat{\mathrm{V}}$$

Design parameters F, G are positive definite matrices, $k > 0$ a small design parameter.

$\dot{L}$ is negative outside a compact set and selecting the gain according to

$$K_{v_{\min}} > \frac{((C_0 + \mathrm{k}C_3^{\ 2}) / 4)(\mathrm{c}_0 + \mathrm{c}_2)}{b_x - q_B}$$

Ensures that the compact set defined by $\| r \| \leq b_r$ is contained in S_r, so that the approximation property holds throughout. This demonstrates the UUB of both $\| r \|$ and $\| \tilde{W}_B \|_F$. The bounds are given as

$$\| \mathrm{r} \| > \frac{(C_0 + \mathrm{k}C_3^{\ 2}) / 4)}{K_{v_{\min}}} \equiv b_r$$

$$\| \tilde{\mathrm{Z}} \|_F > C_3 / 2 + \sqrt{C_0 / k + C_3^{\ 2} / 4} \equiv b_z$$

Details of the proof can be found in [15].

2.4 Discussion

From the closed loop error dynamics it can be seen that it do not contain the desired model parameters in it. This is a unique achievement of this work. All the proofs and bounds are provided for the work in this chapter.

Chapter 3

Simulations

In this chapter the simulation results are provided. The controller designed was tested with a 2 DOF planar robot manipulator. A large class of manipulation task can be represented as profiles in the velocity-force plane [1]. Therefore for the simulation purpose it was considered that the force command was generated by the velocity-force profile in figure which represents a basic robotic motion task. The dynamics of the 2-link arm and the simulations results are provided in the subsequent sections.

3.1 2-DOF Robotic Arm

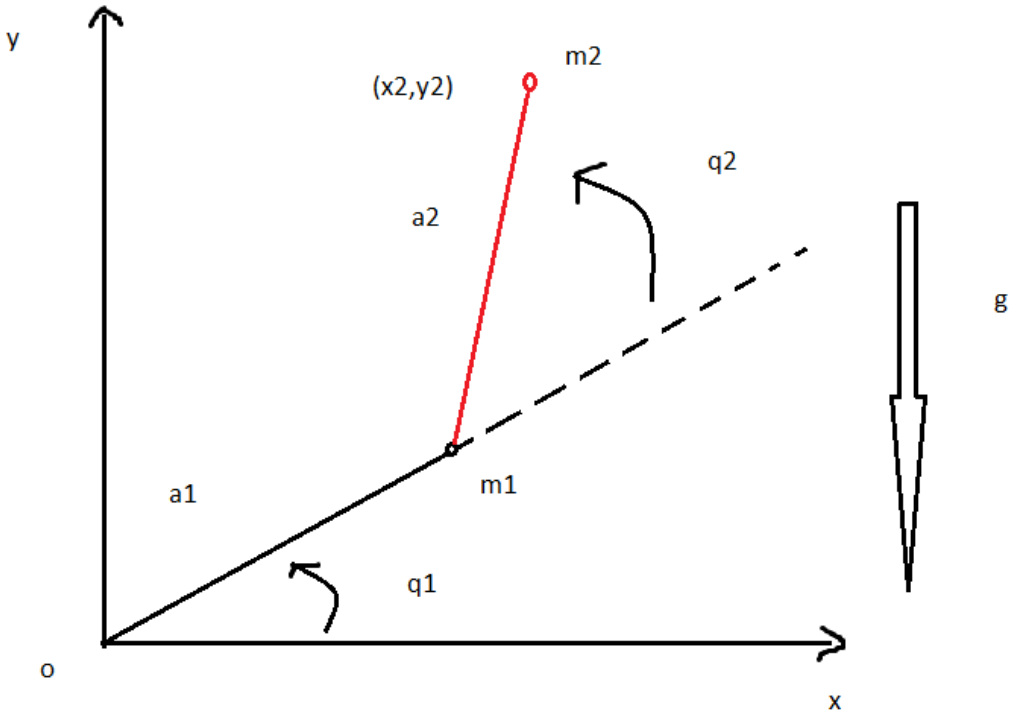

Figure 6: 2-Link Robotic Arm

The 2-DOF robotic arm is shown in the figure above. The lengths of the links are a1 and a2, the mass of the links are m1 and m2 and q1 and q2 are the angular displacements.

3.2 The Dynamics of the Robotic Arm

The arm dynamics used for this work is given below. The details of the derivation of the dynamics can be found in [20]. It is a nonlinear system.

$$\begin{pmatrix} (\mathrm{m}_1+\mathrm{m}_2)\,\mathrm{a}_1{}^2+m_2a^2{}_2+2m_2a_1a_2\cos q_2 & m_2a^2{}_2+m_2a_1a_2\cos q_2 \\ m_2a^2{}_2+m_2a_1a_2\cos q_2 & m_2a^2{}_2 \end{pmatrix}\begin{pmatrix} \ddot{q}_1 \\ \ddot{q}_2 \end{pmatrix}+\begin{pmatrix} -m_2a_1a_2(2\,\dot{\mathrm{q}}_1\dot{\mathrm{q}}_2+\dot{\mathrm{q}}_2^2)\sin\mathrm{q}_2 \\ m_2a_1a_2\,\dot{\mathrm{q}}_1^2\sin\mathrm{q}_2 \end{pmatrix}$$
$$+\begin{pmatrix} (\mathrm{m}_1+\mathrm{m}_2)\,\mathrm{g}\,\mathrm{a}_1\cos q_1+m_2ga_2\cos(\mathrm{q}_1+\mathrm{q}_2) \\ m_2ga_2\cos(\mathrm{q}_1+\mathrm{q}_2) \end{pmatrix}=\begin{pmatrix} \tau_1 \\ \tau_2 \end{pmatrix}$$

(38)

3.3 The Dynamics of the Desired Model

The desired reference model is given below. The robotic system is to fell like this model. By changing the parameter in this model the interaction behavior of the robotic system can be varied.

$$\begin{pmatrix} M & 0 \\ 0 & M \end{pmatrix}\begin{pmatrix} \ddot{q}_{m1} \\ \ddot{q}_{m2} \end{pmatrix}+\begin{pmatrix} D & 0 \\ 0 & D \end{pmatrix}\begin{pmatrix} \dot{q}_{m1} \\ \dot{q}_{m2} \end{pmatrix}+\begin{pmatrix} K & 0 \\ 0 & K \end{pmatrix}=\begin{pmatrix} f_{h1} \\ f_{h2} \end{pmatrix} \tag{39}$$

For the simulation purpose M, D and K are taken as:

M = [2 0; 0 2];

D = [1 0; 0 1];

K = [1 0; 0 1];

3.4 Van der Pol Oscillator

Van der Pol Oscillator is used to generate the forces that are applied as human force during interaction with the robotic system. A large class of manipulation tasks has been represented in velocity-force plane profiles [1]. For that reason the Van der Pol Oscillator has been used to generate the forces that are applied on the robotic system. The equation of the oscillator is given below.

$$\ddot{y} + \alpha(\mathrm{y}^2 - 1)\,\dot{\mathrm{y}} + \mathrm{y} = \mathrm{u}$$

In Brunovsky canonical form:

$$\dot{x}_1 = x_2$$
$$\dot{x}_2 = \alpha(1 - \mathrm{x}_1{}^2)\,\mathrm{x}_2 - x_1 + u$$

where the states x_1 is position and x_2 velocity.

3.5 Tuning Algorithm

The following controller is used with the given control input and neural network weight tuning algorithm for simulation.

Control input:

$$\tau = \hat{W}^T \sigma(\hat{\mathrm{V}}^T \mathrm{x}) + \mathrm{K}_v\, r - v$$

Robustifying Signal:

$$v(\mathrm{t}) = -\mathrm{K}_z(\| \hat{\mathrm{Z}} \|_F + \mathrm{Z}_B)\,\mathrm{r}$$

NN Weight/ Threshold Tuning Algorithms:

$$\dot{\hat{W}} = F\hat{\sigma}r^T - F\hat{\sigma}'\hat{V}^T xr^T - kF \| \mathrm{r} \| \hat{\mathrm{W}}$$

$$\dot{\hat{V}} = Gx(\hat{\sigma}^{\mathrm{T}} \hat{\mathrm{W}}\mathrm{r})^T - kG \| \mathrm{r} \| \hat{\mathrm{V}}$$

Design parameters F, G are positive definite matrices, $k > 0$ a small design parameter.

3.6 Simulation Results

All the simulation results are provided in this section. The forces that are applied on the robotic system, the error, and the actual and desired responses all are provided under this section.

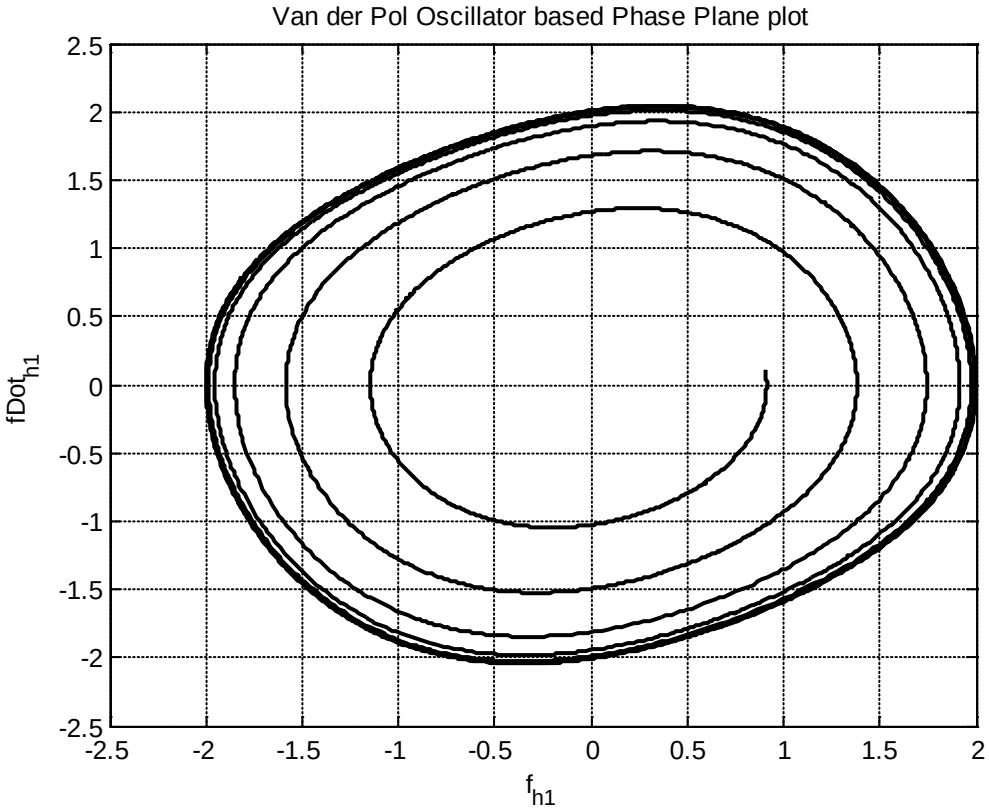

Figure 7: Van der Pol Oscillator Phase Plane Plot

The above figure shows the phase plane plot of the Van der Pol Oscillator. This is force that is used as the human force.

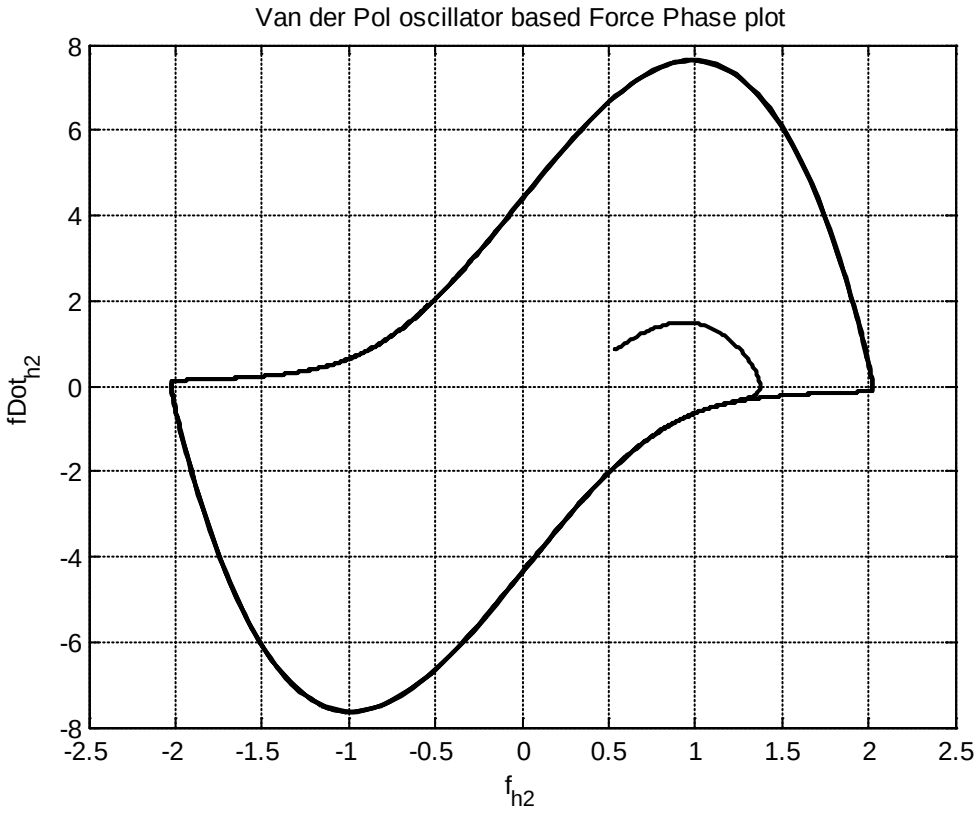

Figure 8: Van der Pol Oscillator based Force Phase Plot

The above figure shows the force phase plot of the Van der Pol Oscillator.

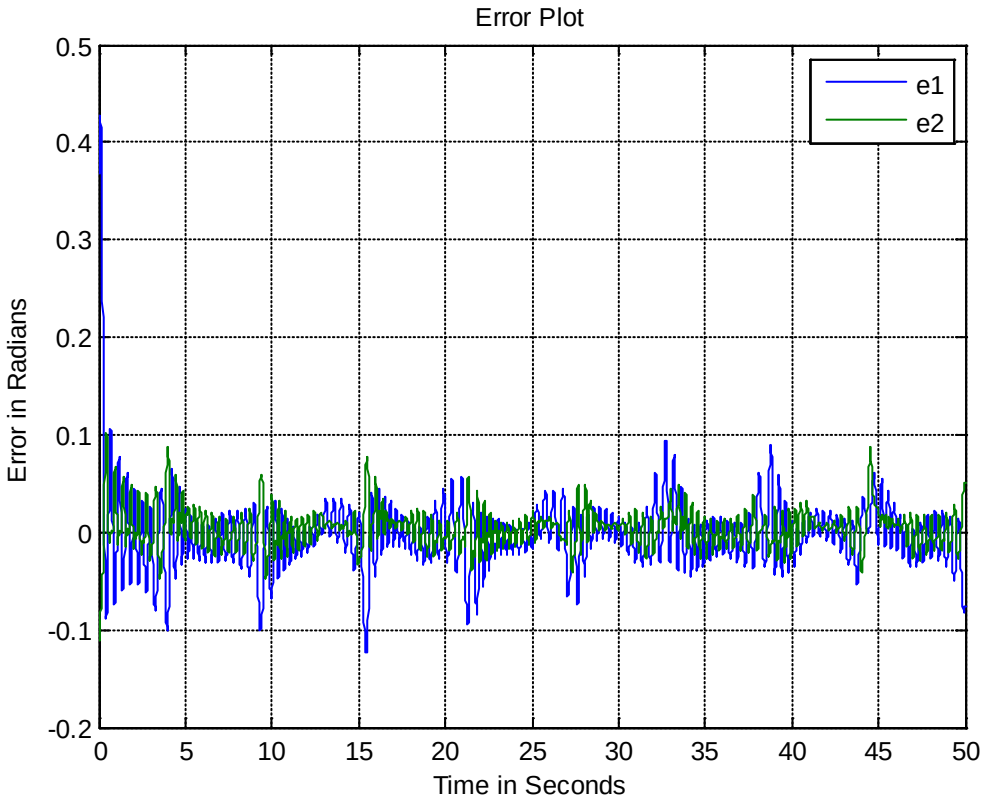

Figure 9: Error Plot

The above figure shows the error between the actual joint angles and the desired one from the model. It provides error plot for both the joints. A norm of 3.4314 on error was found for this simulation. It can be seen that the error is near the zero mark.

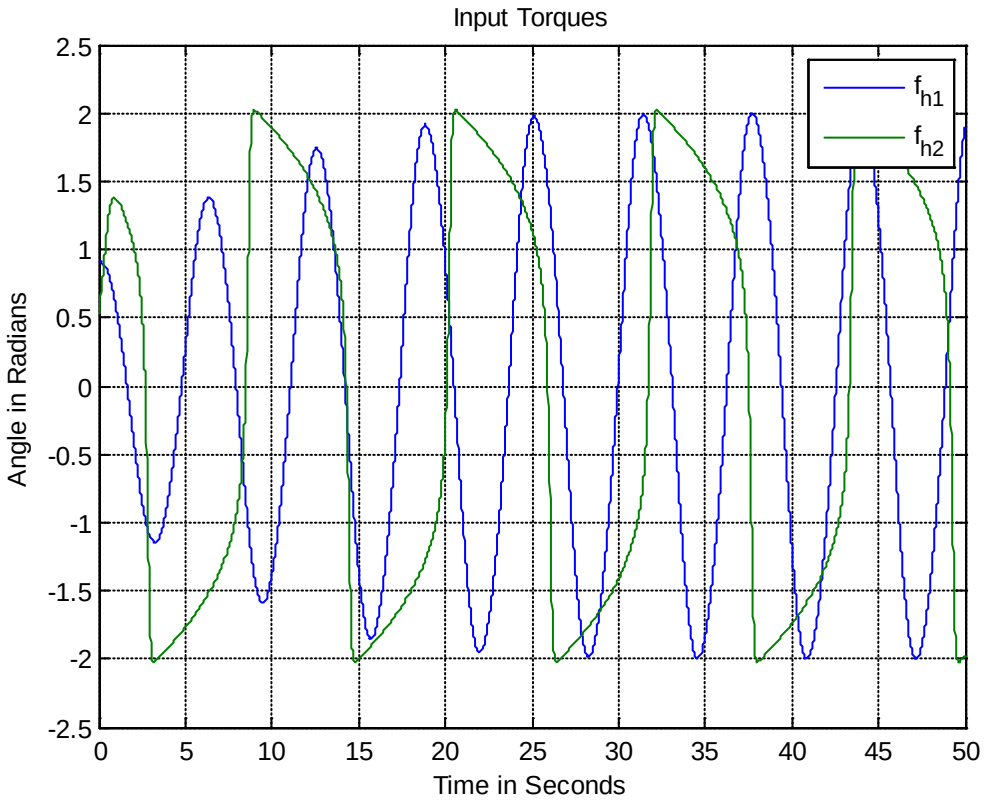

Figure 10: The Input Torques to the System

Figure 8 shows the input torques that was provided to the system. The forces applied by the Van der Pol oscillator are transformed to torques using the Jacobian matrix. This torques drives the joint angles.

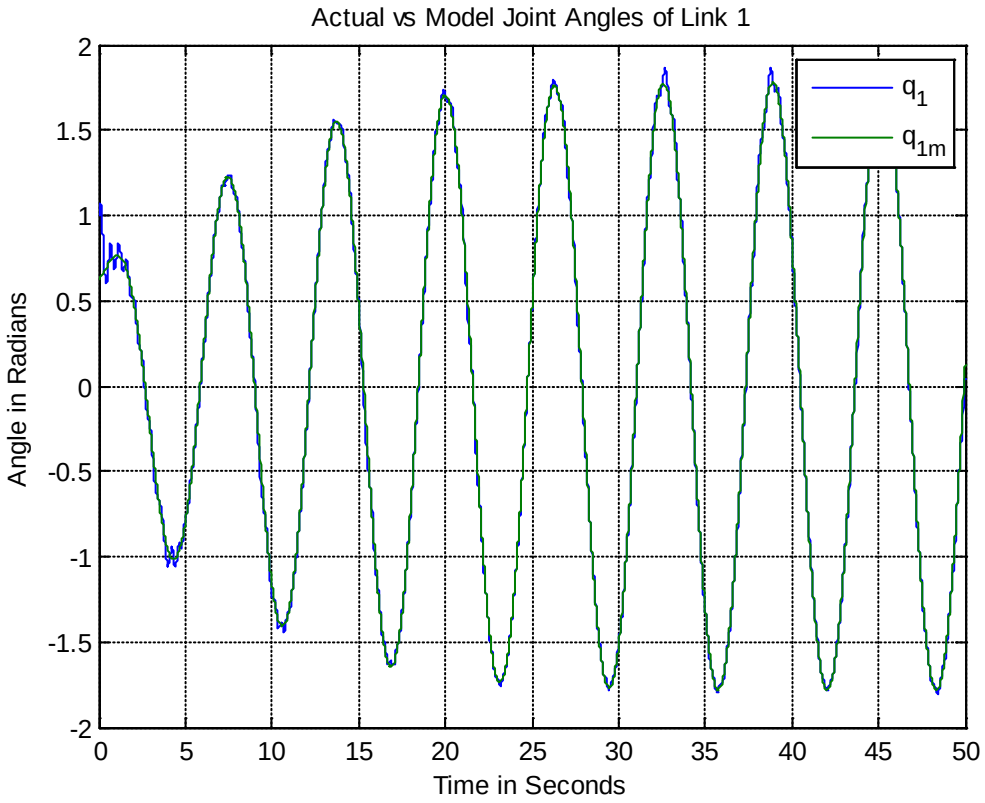

Figure 11: Actual and Desired Model Angles for Joint 1

The above figure shows the actual and the model joint angles of link 1 of the robot in figure 6. The blue color plot is the actual joint angle and the green color plot is the joint angles of the model. It can be seen that they pretty much follow each other showing that the designed controller is working perfectly.

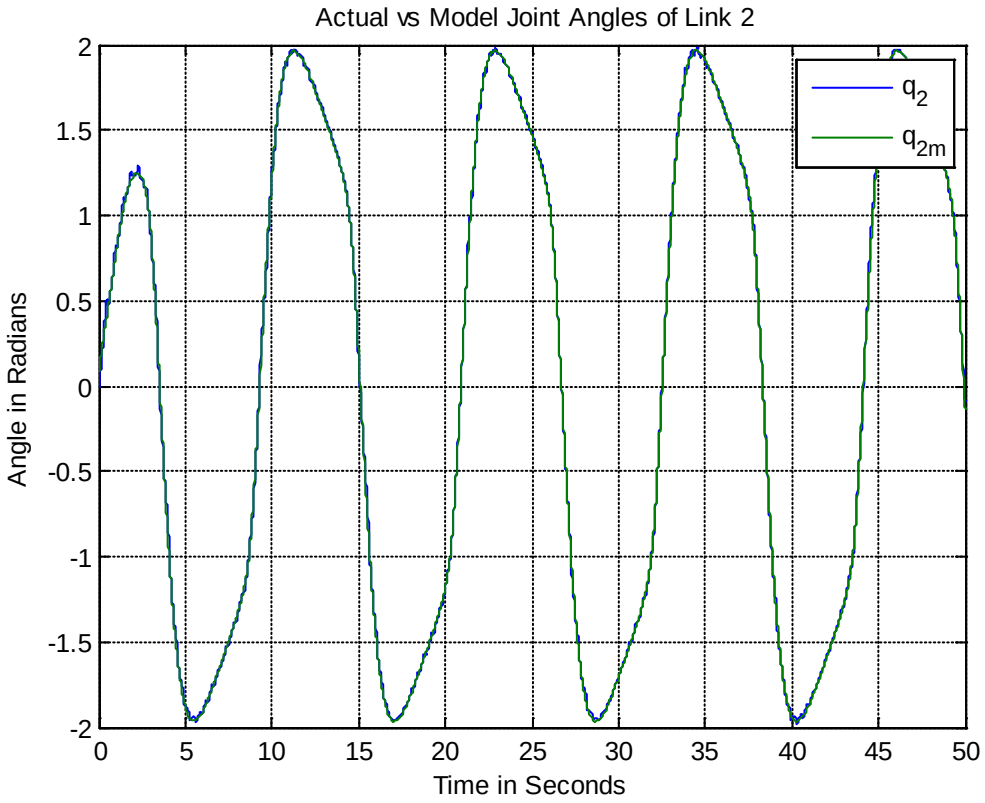

Figure 12: Actual and Desired Model Angles for Joint 2

The above figure shows the actual and the model joint angles of link 2 of the robot in figure 6. The blue color plot is the actual joint angle and the green color plot is the joint angles of the model. It can be seen that they pretty much follow each other showing that the designed controller is working perfectly.

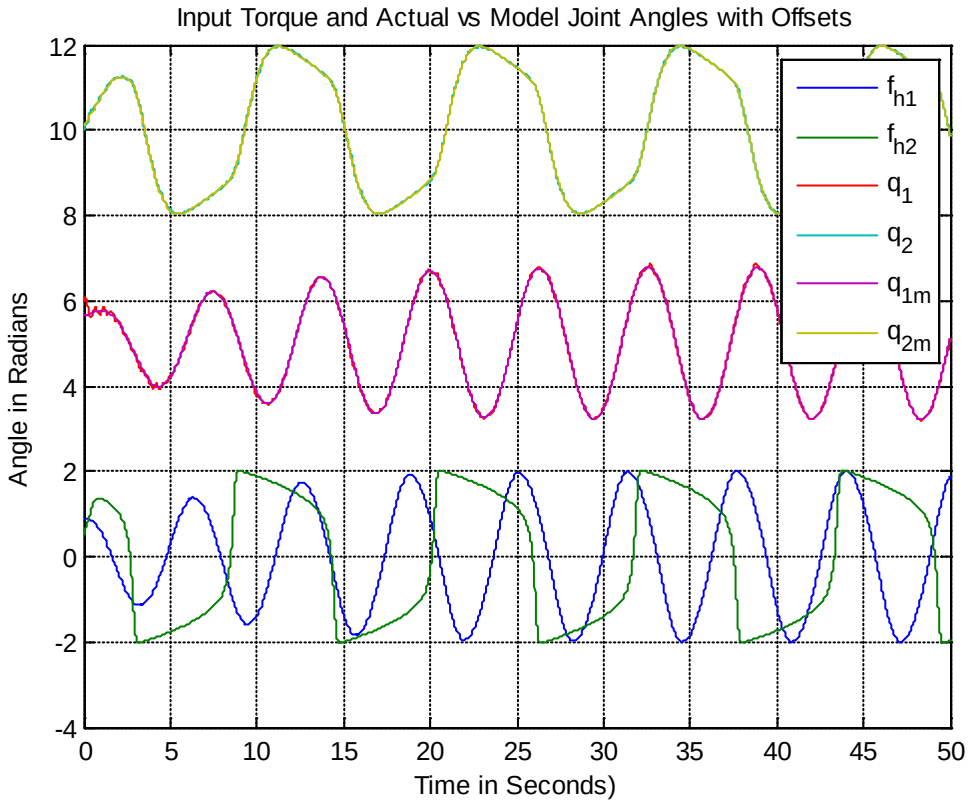

Figure 13: Actual and Desired Model Angles with Offsets

The input torque and actual and model joint angles with offsets are also plotted. The figure above shows the results.

3.7 Discussion:

This chapter contains the details of the simulation results that are carried out to prove the effectiveness of the designed controller. It can be clearly seen from the figure 11 and 12 that the actual joint angles and the desired model coincide. MATLAB is used to carry out the simulations.

Chapter 4

The Outer Loop Design

If a human is asked to drive or control a plant and is given a condition that the combined behavior of him and the plant should follow the response of a desired model then how the human should perform this work. It is logical to think that the human will see the current output of the desired model and check with its combined response with the plant and then estimate an error and based on the error will change its actions so as to minimize that error and improve the overall performance. An according to [25] modeling human control characteristic is complex as various kinds of compensators are needed. However, under limited operation condition a linear model plus a delay [26] can be used to represent human control characteristics. The famous cross over model says that the transfer function of the human in a human in the loop system become accustomed so as to keep the complete system unchanged under the variation of the controlled system dynamics. The work in [27] found validity of such model through a juggling task using haptic test device.

In this chapter the details of the outer loop formation is provided. Two different situations are taken into consideration for this work. At first, it is assumed that the human model is known and in the second the human model is approximated by designing an observer. At the end the structure is modified to make it more realistic. In all cases the concept of crossover model is used. That is the human and the robotic system is made to look like a first order system. Theories developed in [28] are used for the derivations. The mathematical formulations of the different contexts are provided in this chapter as well.

4.1 The Control Structure

Model reference adaptive systems are continuously being studied and it has made way to numerous applications. In [29] the different model reference control structures were studied. The two most commonly used ones are structure with a series reference model and structure with parallel reference model. The series reference model structure used for this work is given below.

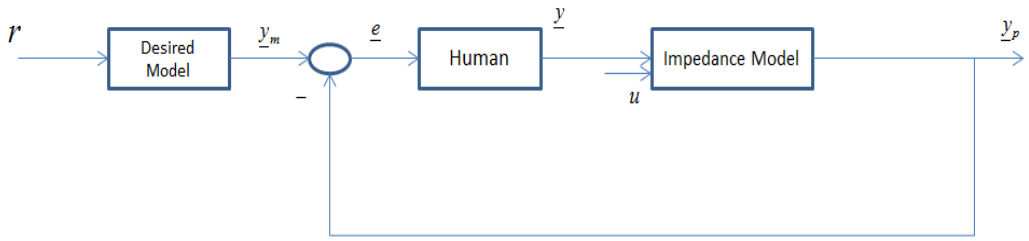

Figure 14: The General Control Structure for the Outer Loop

This structure assumes the human acts based on the error between the plant and model's output not with the input that drives the reference model. In reality, the human rectify or correct its actions based on what he wants and what he is getting for his current actions. So the feedback in the system provides with that information. The inner loop (neuroadaptive controller developed in chapter 2) should be inside the impedance model block.

4.2 With Human Model Known

In this section the human model is assumed to be known. The model is taken as [4]. In reality this model should vary from person to person and must be identified during the operation to assist the person in doing some work.

4.2.1 Mathematical Derivations

In this section the mathematical derivations of the outer loop for the above case is provided.

For the control system the following subsystems are defined.

Model

$$\dot{y}_m = -a_m y_m + b_m r \tag{41}$$

Plant/ Inner Loop Impedance Model

$$\dot{y}_p = -a_n y_p + b_n u \tag{42}$$

Human

$$\dot{y} = -ay + be \tag{43}$$

Defining the error and the control law as

Error

$$e = y_m - y_p \tag{44}$$

Control law

$$u = -\theta_1 y - \theta_2 y_p - \theta_3 r \tag{45}$$

Differentiating the error with respect to time

$$\begin{aligned}
\dot{e} &= \dot{y}_m - \dot{y}_p \\
&= -a_m y_m + b_m r + a_n y_p - b_n u \\
&= -a_m y_m + b_m r + a_n y_p - b_n(-\theta_1 y - \theta_2 y_p - \theta_3 r) + \mathrm{a}_m \mathrm{y}_p - \mathrm{a}_m \mathrm{y}_p \\
&= -\mathrm{a}_m e + \mathrm{b}_n \theta_1 y + \mathrm{y}_p(\mathrm{b}_n \theta_2 + \mathrm{a}_n - \mathrm{a}_m) + r(\mathrm{b}_m + \mathrm{b}_n \theta_3)
\end{aligned}$$

Selecting a Layapunov candidate function

$$v = \frac{1}{2}\gamma e^2 + \frac{1}{2b_n\gamma_1}(b_n\theta_1)^2 + \frac{1}{2b_n\gamma_2}(b_n\theta_2 + a_n - \mathrm{a}_m)^2 + \frac{1}{2b_n\gamma_3}(\mathrm{b}_m + b_n\theta_3)^2$$

Therefore, differentiating the above function

$$\dot{v} = \gamma e\dot{e} + \frac{1}{\gamma_1}\dot{\theta}_1(b_n\theta_1) + \frac{1}{\gamma_2}\dot{\theta}_2(b_n\theta_2 + a_n - \mathrm{a}_m) + \frac{1}{\gamma_3}\dot{\theta}_3(\mathrm{b}_m + b_n\theta_3)$$

Now substituting $\dot{e}$ and $\dot{\tilde{y}}$ in the above equation and simplifying, the function obtained is

$$\dot{v} = -a_m\gamma e^2 + b_n\theta_1(\gamma\,\mathrm{ey} + \frac{1}{\gamma_1}\dot{\theta}_1) + (b_n\theta_2 + a_n - \mathrm{a}_m)(\gamma\,\mathrm{e}\,y_p + \frac{1}{\gamma_2}\dot{\theta}_2) + (\mathrm{b}_m + b_n\theta_3)(\gamma\,\mathrm{er} + \frac{1}{\gamma_3}\dot{\theta}_3)$$

Now selecting

$$\dot{\theta}_1 = -\gamma ey\gamma_1$$
$$\dot{\theta}_2 = -\gamma ey_p\gamma_2$$
$$\dot{\theta}_3 = -\gamma er\gamma_3$$

$\dot{v}$ becomes

$$\dot{v} = -a_m\gamma e^2 \qquad (46)$$

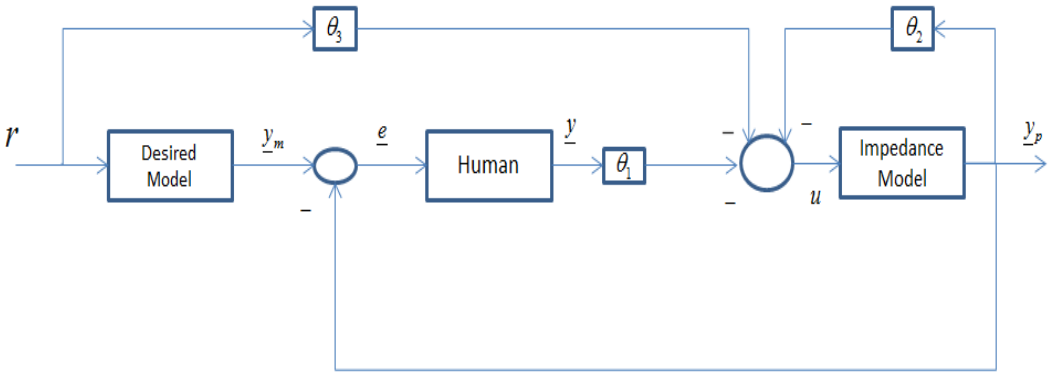

Figure 15: The Outer Loop with the Parameters

4.2.2 Simulation Results

In this section the simulation results are provided. For the purpose of simulation the following systems with given transfer functions are considered.

Human

$$H(s) = \frac{3}{s+2}$$

Impedance Model

$$P(s) = \frac{5}{s+4}$$

Reference Model

$$R(s) = \frac{4}{s+3}$$

For values of g1=g2=g3=1 the following results are obtained.

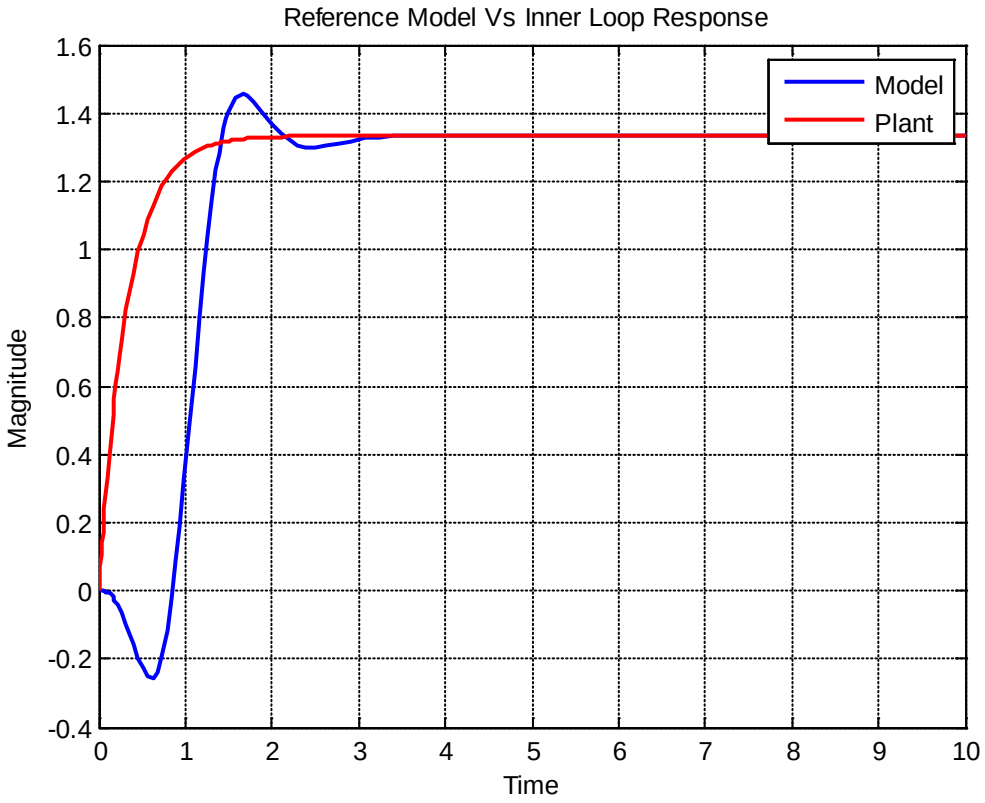

Figure 16: Reference Model and Plant Response

From the above diagram it can be seen that both the responses matched each other after a certain period of time showing that all the update laws are working fine.

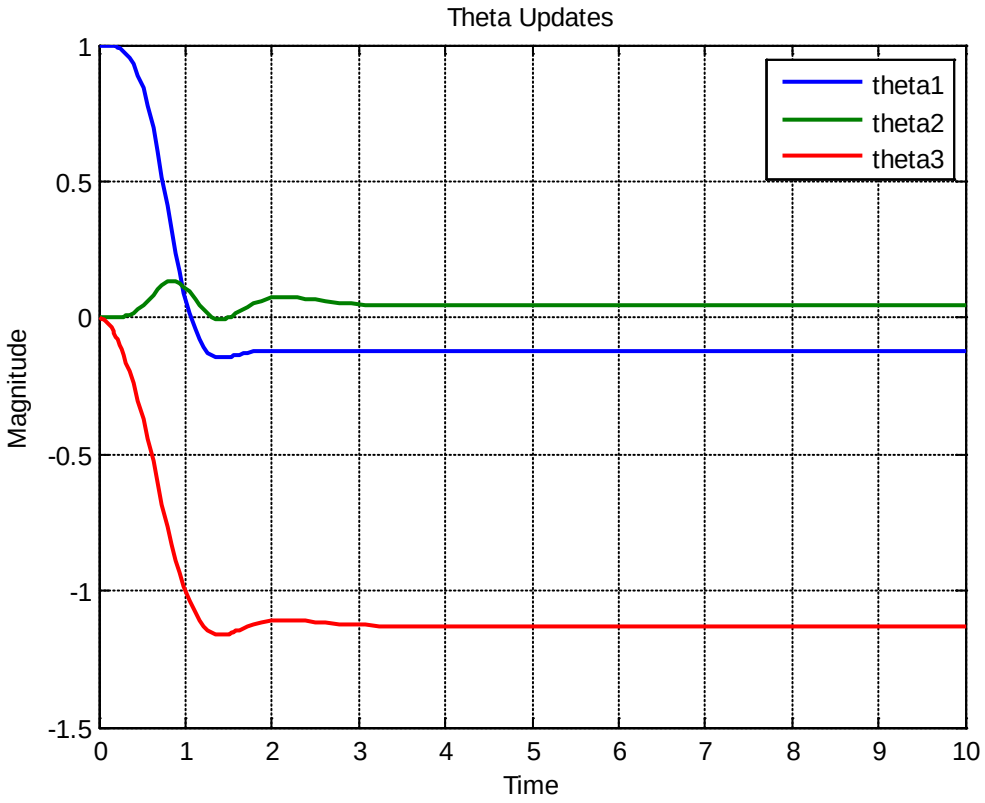

Figure 17: Parameter Updates

The above diagram shows the parameter updates with time. It can be seen that all the parameter reaches a steady value after a while indicating the desired outcomes has been reached.

4.3 With Human Model Unknown

In this section the human model is unknown. As the human model should vary for every different individual it is very important that the operator's dynamics is found out. In order to tackle this problem and observer is designed which estimates the dynamics of the human. A similar approach as above is used to design the outer loop for this case.

4.3.1 Mathematical Derivations

For the control system the following subsystems are defined.

Model

$$\dot{y}_m = -a_m y_m + b_m r \tag{47}$$

Plant/ Inner Loop Impedance Model

$$\dot{y}_p = -a_n y_p + b_n u \tag{48}$$

Human

$$\dot{y} = -ay + be \tag{49}$$

Observer

$$\dot{\hat{y}} = -\hat{a}\hat{y} + \hat{b}e \tag{50}$$

The error between the observer and the observed human model is

$$\begin{aligned}
\dot{\tilde{y}} &= \dot{y} - \dot{\hat{y}} \\
&= -ay + be + \hat{a}\hat{y} - \hat{b}e \\
&= -ay + \hat{a}\hat{y} + (\mathrm{b} - \hat{\mathrm{b}})\,\mathrm{e} \\
&= -ay + \hat{a}\hat{y} + (\mathrm{b} - \hat{\mathrm{b}})\,\mathrm{e} + a\hat{y} - a\hat{y} \\
&= -a(\mathrm{y} - \hat{\mathrm{y}}) + \hat{y}(\hat{\mathrm{a}} - \mathrm{a}) + (\mathrm{b} - \hat{\mathrm{b}})\,\mathrm{e}
\end{aligned}$$

$$\dot{\tilde{y}} = -a\,\tilde{\mathrm{y}} + \hat{y}\,\tilde{\mathrm{a}} + (-\tilde{\mathrm{b}})\,\mathrm{e} \tag{51}$$

Defining the error and the control law as

Error

$$e = y_m - y_p \tag{52}$$

Control law

$$u = -\theta_1 \dot{\hat{y}} - \theta_2 y_p - \theta_3 \hat{y} - \theta_4 r \tag{53}$$

Differentiating the error with respect to time

$$\begin{aligned}
\dot{e} &= \dot{y}_m - \dot{y}_p \\
&= -a_m y_m + b_m r + a_n y_p - b_n u \\
&= -a_m y_m + b_m r + a_n y_p - b_n(-\theta_1 \dot{\hat{y}} - \theta_2 y_p - \theta_3 \hat{y} - \theta_4 r) + \mathrm{a}_m \mathrm{y}_p - \mathrm{a}_m \mathrm{y}_p \\
&= -\mathrm{a}_m e + r(\mathrm{b}_m + \mathrm{b}_n \theta_4) - \mathrm{y}_p(-\mathrm{b}_n \theta_2 + \mathrm{a}_m - \mathrm{a}_n) - \mathrm{b}_n \hat{\mathrm{b}} \theta_1 \mathrm{x} - \mathrm{b}_n \hat{\mathrm{y}}(\hat{\mathrm{a}} \theta_1 - \theta_3)
\end{aligned}$$

Selecting a Layapunov candidate function

$$v = \frac{1}{2}\gamma e^2 + \frac{1}{2b_n \hat{b}\gamma_1}(b_n \hat{b}\theta_1)^2 + \frac{1}{2b_n \gamma_2}(-b_n \theta_2 + \mathrm{a}_m - a_n)^2 + \frac{1}{2\gamma_3}(\hat{\mathrm{a}}\theta_1 - \theta_3)^2 + \frac{1}{2b_n \gamma_4}(\mathrm{b}_m + b_n \theta_4)^2$$
$$+ \frac{1}{2}\tilde{y}^2 + \frac{1}{2\gamma_5}(\hat{\mathrm{a}} - a)^2 + \frac{1}{2\gamma_6}(\mathrm{b} - \hat{b})^2$$

Therefore, differentiating the above function

$$\dot{v} = \gamma e \dot{e} + \frac{1}{\gamma_1}\dot{\theta}_1(b_n \hat{b}\theta_1) - \frac{1}{\gamma_2}\dot{\theta}_2(-b_n \theta_2 + \mathrm{a}_m - a_n) + \frac{1}{\gamma_3}(\hat{\mathrm{a}}\theta_1 - \theta_3)(\hat{\mathrm{a}}\dot{\theta}_1 - \theta_3) + \frac{1}{\gamma_4}\dot{\theta}_4(\mathrm{b}_m + b_n \theta_4)$$
$$+ \tilde{y}\dot{\tilde{y}} + \frac{1}{\gamma_5}(\hat{\mathrm{a}} - a)\dot{\hat{\mathrm{a}}} + \frac{1}{\gamma_6}(\mathrm{b} - \hat{b})\dot{\hat{b}}$$

Now substituting $\dot{e}$ and $\dot{\tilde{y}}$ in the above equation and simplifying, the function obtained is

$$\dot{v} = -a_m \gamma e^2 + (\mathrm{b}_m + b_n\theta_4)(\gamma\,\mathrm{e} + \frac{1}{\gamma_4}\dot{\theta}_4) + (-b_n\theta_2 + \mathrm{a}_m - a_n)(-\gamma\,\mathrm{e}\,y_p - \frac{1}{\gamma_2}\dot{\theta}_2) + (b_n\hat{b}\theta_1)(\gamma\,\mathrm{e}\,x + \frac{1}{\gamma_1}\dot{\theta}_1)$$

$$+(\hat{\mathrm{a}}\,\theta_1 - \theta_3)(-\gamma\,\mathrm{e}\,b_n\,\hat{\mathrm{y}} + \frac{1}{\gamma_3}((\hat{\mathrm{a}}\,\dot{\theta}_1 - \theta_3)) - \mathrm{a}\tilde{\mathrm{y}}^2 + \tilde{a}(\hat{y}\tilde{y} + \frac{1}{\gamma_5}\dot{\hat{\mathrm{a}}}) - \tilde{\mathrm{b}}(\tilde{\mathrm{y}}\mathrm{x} - \frac{1}{\gamma_6}\dot{\hat{b}})$$

Now selecting

$$\dot{\theta}_1 = -\gamma ex\gamma_1$$
$$\dot{\theta}_2 = -\gamma e y_p \gamma_2$$
$$\dot{\theta}_3 = -\hat{a}\gamma ex\gamma_1 - \gamma e b_n \hat{y}\gamma_3$$
$$\dot{\theta}_4 = -\gamma e\gamma_4$$
$$\dot{\hat{a}} = -\hat{y}\tilde{y}\gamma_5$$
$$\dot{\hat{b}} = \tilde{y}x\gamma_6$$

$\dot{v}$ becomes

$$\dot{v} = -a_m \gamma e^2 - a\tilde{y}^2 \tag{54}$$

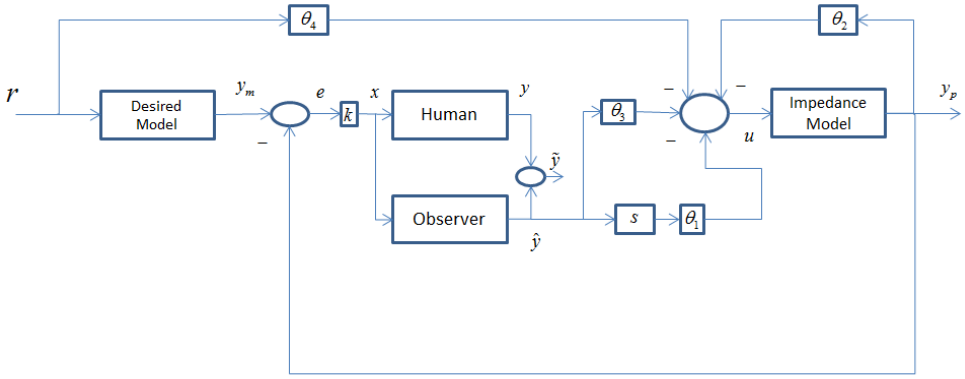

Figure 18: The Outer Loop with the Parameters

4.3.2 Simulation Results

In this section the simulation results are provided. For the purpose of simulation the following systems with given transfer functions are considered.

Human

$$H(\mathrm{s}) = \frac{3}{s+2}$$

Impedance Model

$$P(\mathrm{s}) = \frac{5}{s+4}$$

Reference Model

$$R(\mathrm{s}) = \frac{4}{s+3}$$

For values of g1=g2=g3=g4=1 and g5=g6=100 the following results are obtained.

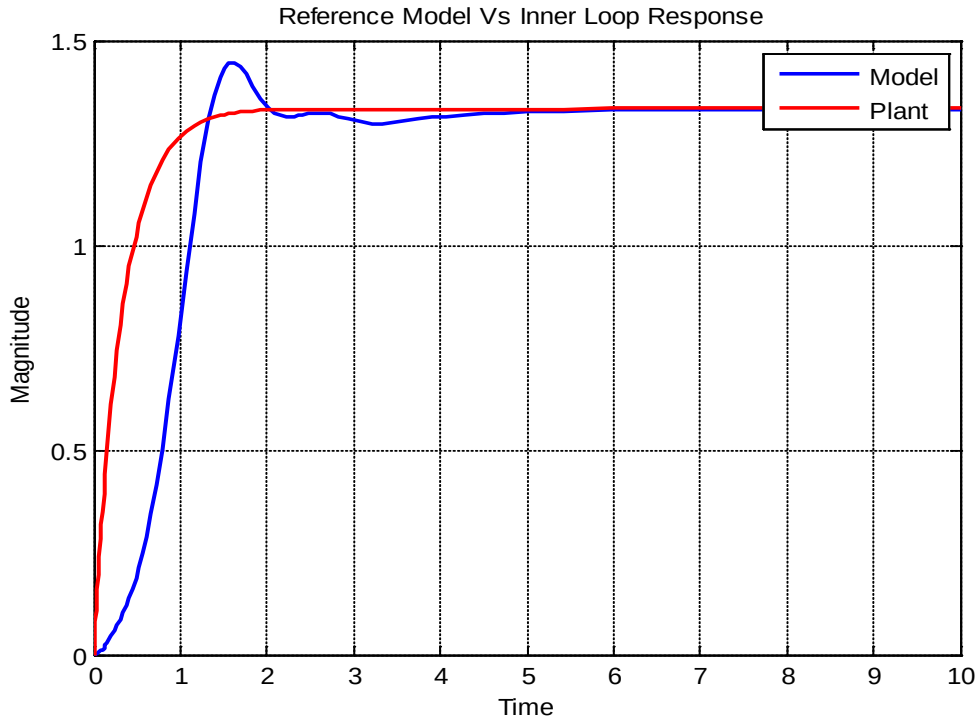

Figure 19: Reference Model Vs Plant Response

From the above diagram it can be seen that both the responses matched each other after a certain period of time showing that all the update laws are working fine.

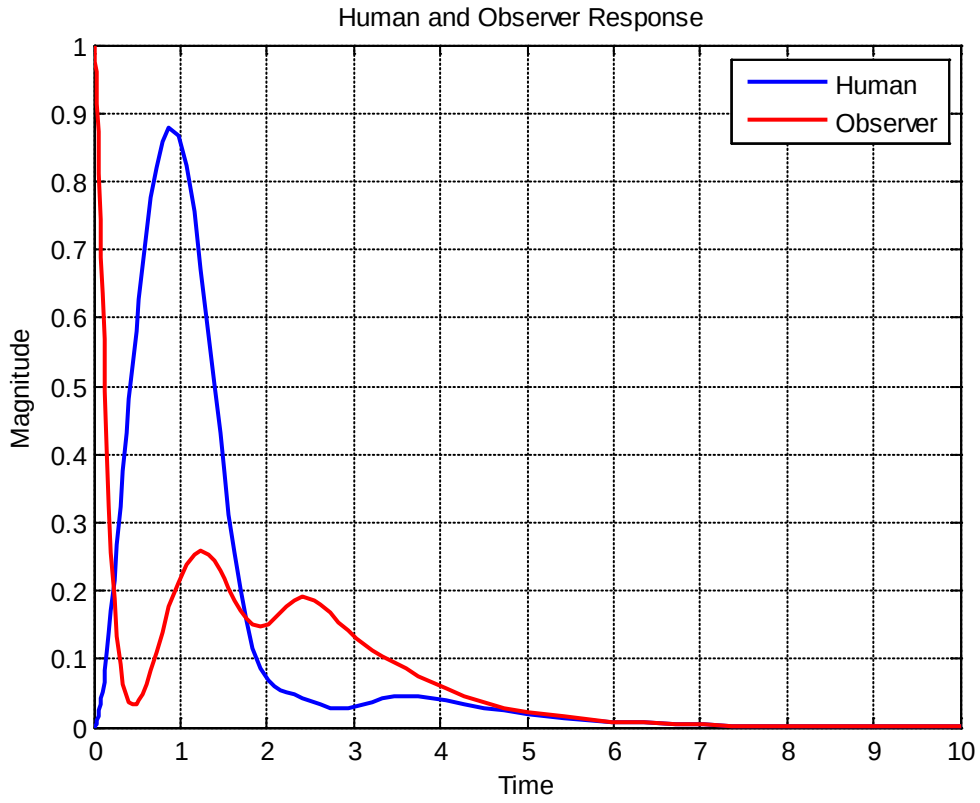

Figure 20: Human and Observer Response

From figure 20, It can be seen that the human and the observer responses matches after 6 seconds. This tells us that the error between the two has diminished.

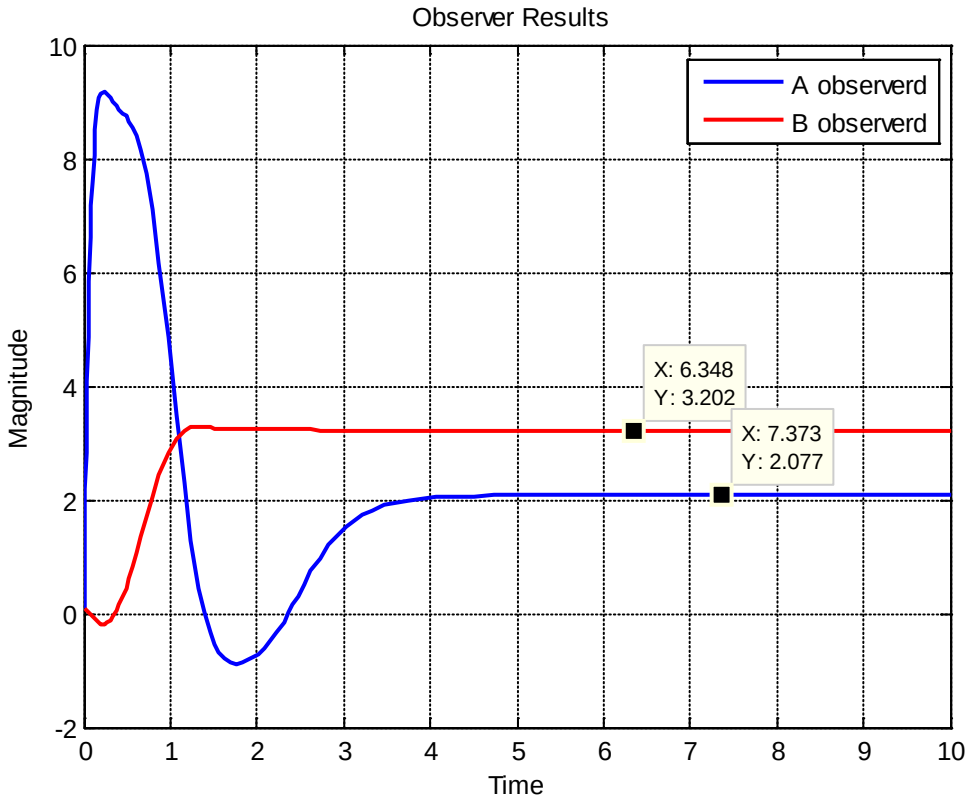

Figure 21: Observer Results

From the above figure it can be seen that the observer reached certain values and settled. The values reached are 3 and 2 which are the values from the Human transfer function. This shows that the observer is working properly.

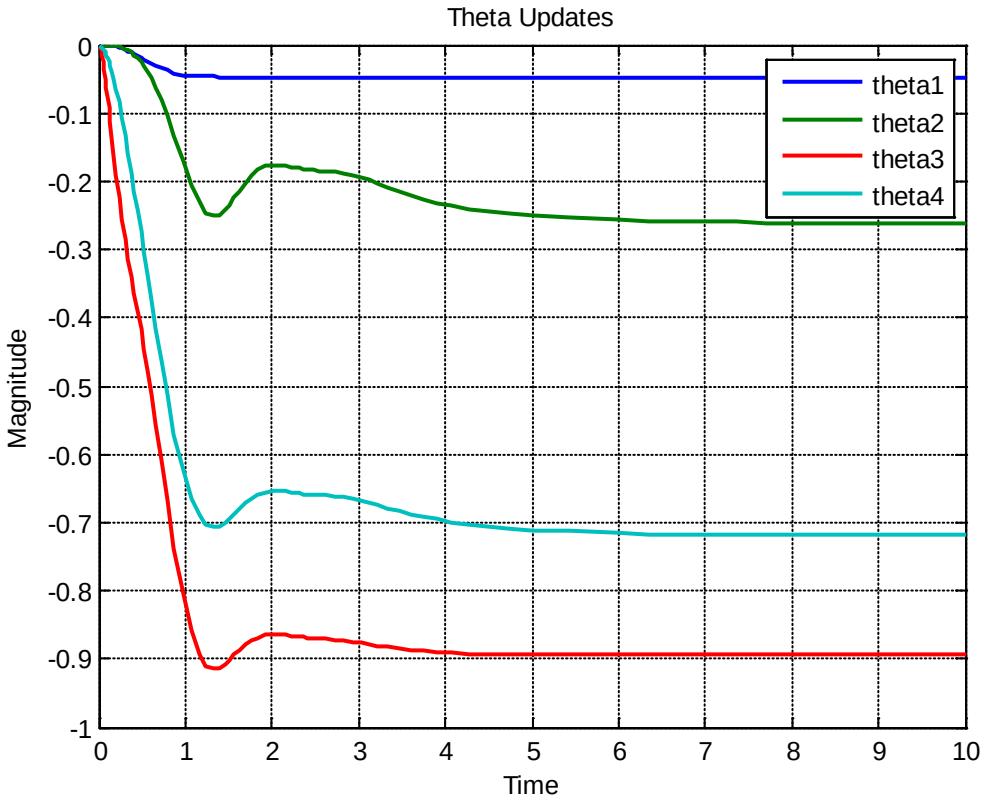

Figure 22: Parameter Updates

The above diagram shows the parameter updates with time. It can be seen that all the parameter reaches a steady value after a while indicating the desired outcomes has been reached. In this case there are four parameters instead of three in previous case.

4.4 Modified System With Human Model Unknown

In the previous two structures the human acted based on the error it sees between the desired and the actual outputs of the plant. But had no information about the reference signal which drives the model. This could be taken as a drawback as the human should have some information about the reference signal. To make the system

realistic the human should have information about both the reference signal and the error. In order to overcome this problem the existing system is modified. The modified system is given below.

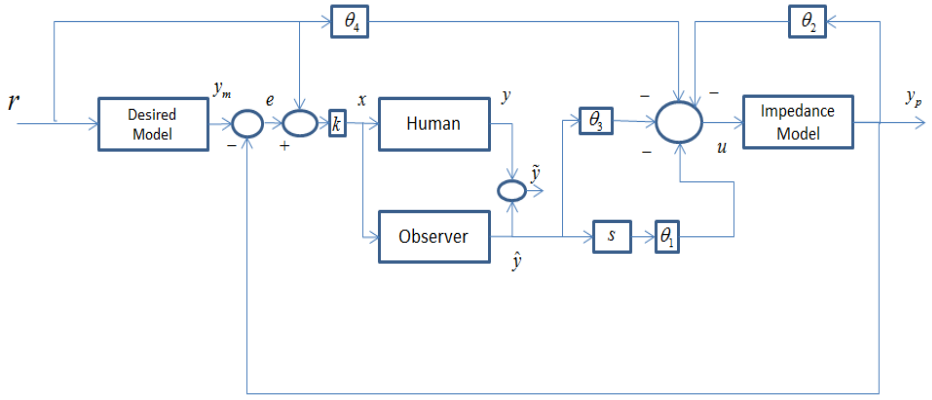

Figure 23: Modified System

4.4.1 Mathematical Derivations

In this section the mathematical derivations of the modified system are provided. For the control system the following subsystems are defined.

Model

$$\dot{y}_m = -a_m y_m + b_m r \tag{55}$$

Plant/ Inner Loop Impedance Model

$$\dot{y}_p = -a_n y_p + b_n u \tag{56}$$

Human

$$\dot{y} = -ay + b(e + r) \tag{57}$$

Observer

$$\dot{\hat{y}} = -\hat{a}\hat{y} + \hat{b}(e + r) \tag{58}$$

The signal $e + r$ is taken as x. The error between the observer and the observed human model is

$$\begin{aligned}
\dot{\tilde{y}} &= \dot{y} - \dot{\hat{y}} \\
&= -ay + bx + \hat{a}\hat{y} - \hat{b}x \\
&= -ay + \hat{a}\hat{y} + (\mathrm{b} - \hat{\mathrm{b}})\,\mathrm{x} \\
&= -ay + \hat{a}\hat{y} + (\mathrm{b} - \hat{\mathrm{b}})\,\mathrm{x} + a\hat{y} - a\hat{y} \\
&= -a(\mathrm{y} - \hat{\mathrm{y}}) + \hat{y}(\hat{\mathrm{a}} - \mathrm{a}) + (\mathrm{b} - \hat{\mathrm{b}})\,\mathrm{x}
\end{aligned}$$

$$\dot{\tilde{y}} = -a\,\tilde{\mathrm{y}} + \hat{y}\,\tilde{\mathrm{a}} + (-\tilde{\mathrm{b}})\,\mathrm{x} \tag{59}$$

The derivations is done as before and the following update laws are found

$$\begin{aligned}
\dot{\theta}_1 &= -\gamma e x \gamma_1 \\
\dot{\theta}_2 &= -\gamma e y_p \gamma_2 \\
\dot{\theta}_3 &= -\hat{a}\gamma e x \gamma_1 - \gamma e b_n \hat{y} \gamma_3 \\
\dot{\theta}_4 &= -\gamma e \gamma_4 \\
\dot{\hat{a}} &= -\hat{y}\tilde{y}\gamma_5 \\
\dot{\hat{b}} &= \tilde{y} x \gamma_6
\end{aligned}$$

4.4.2 Simulation Results

In this section the simulation results are provided. For the purpose of simulation the systems with same transfer functions as in section 4.3.2 are taken.

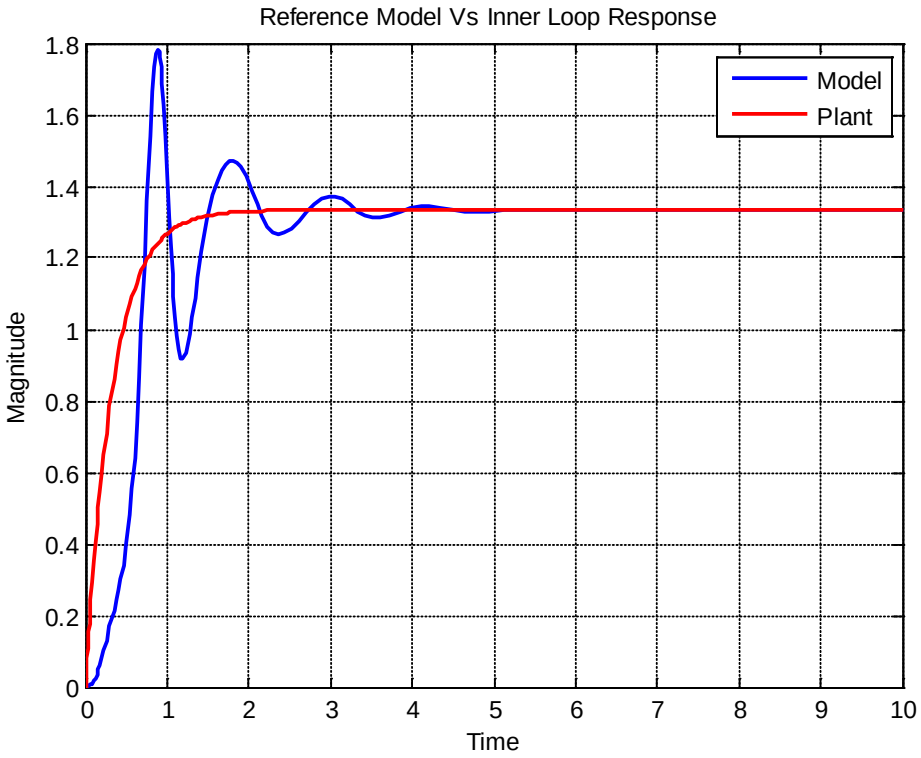

Figure 24: Model Vs Plant Response

The responses on the above diagram matches and showing that the goal is achieved.

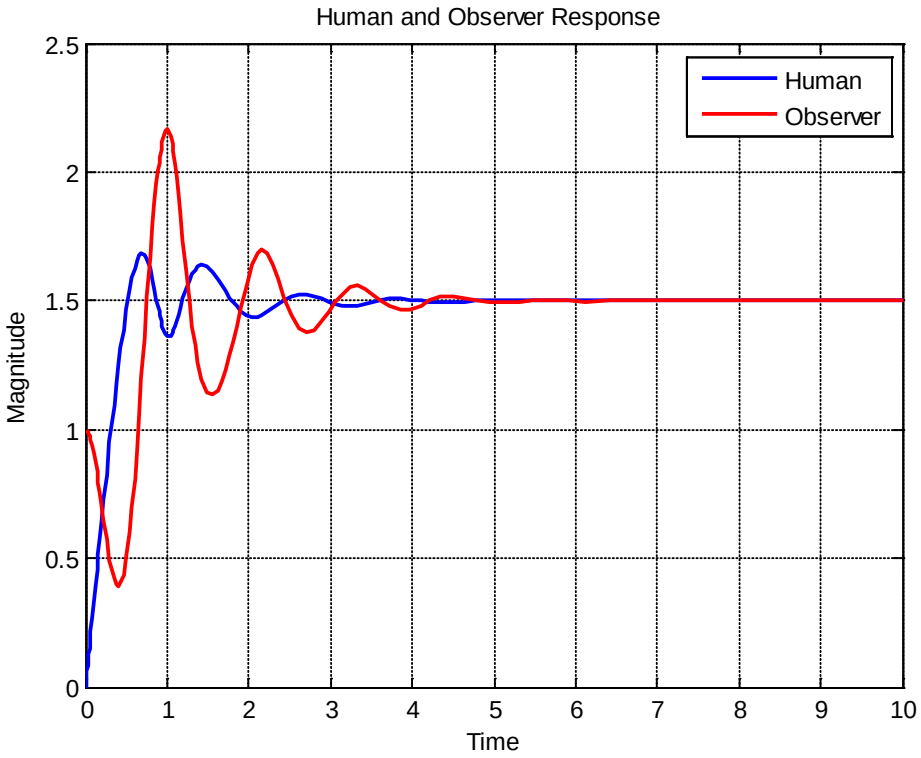

Figure 25: Human and Observer Response

The human and the observer responses becomes same after a certain period of time indicating that the observer is working properly.

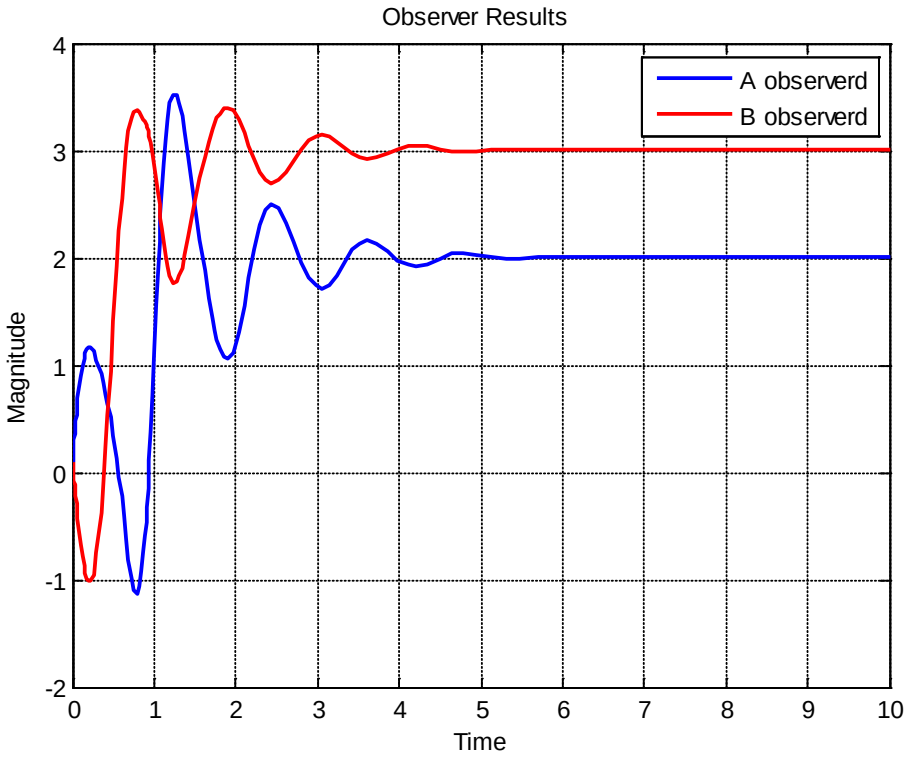

Figure 26: Observer Results

From the above diagram it can be seen that the parameters of the human have been properly found out as the desired vales are reached at steady state. Also from figure 27, it can be seen that the parameter updates reaches a steady state values showing all the update equations are working properly.

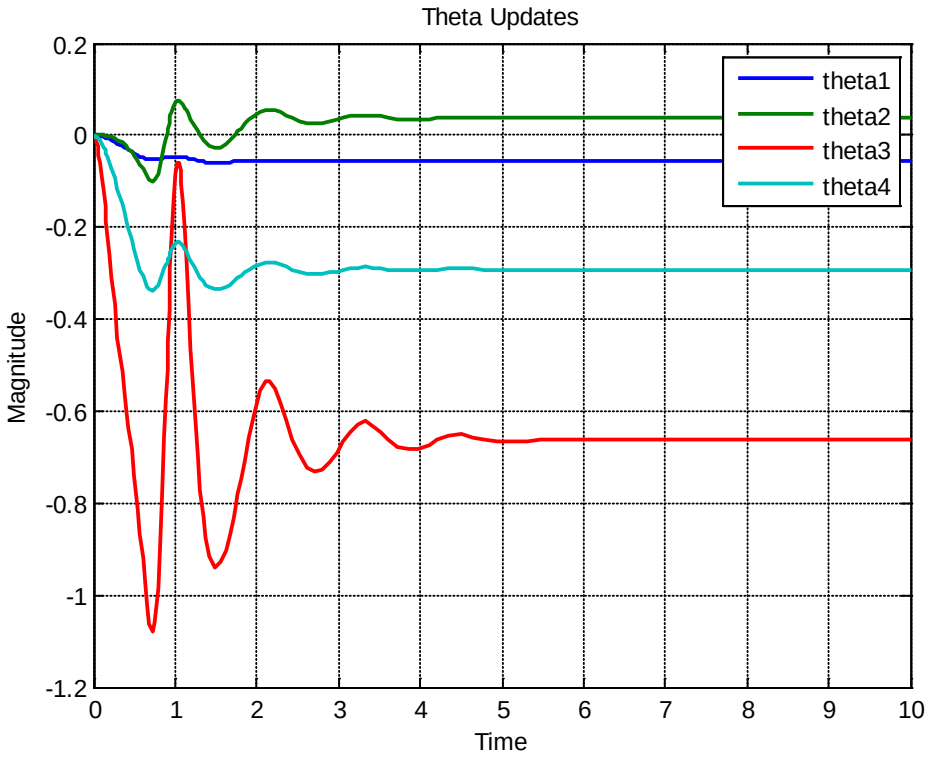

Figure 27: Parameter Updates

4.5 Discussion

In this chapter the outer loop is designed using series model reference control structure. The outer-loop controller tunes the impedance model so that the robot system assists humans with varying levels of skill to achieve task-specific objectives. The crossover model concept is used.

Chapter 5

Conclusion and Future Work

Research in the areas of assistive robotics becomes more and more complicated. The primary reason is that the design must guarantee safety so that the robots can be introduced in a working environment with humans. Also to develop such intelligent robots capable of such fine manipulation lots of human characteristics needs to be modelled. Modelling human characteristics remains an ever challenging task with current state of robotic research. However, significant amount of work is being done and advancement of technology in this field is certain.

This thesis can be taken as having two parts. In first, a novel neuro-adaptive controller is designed. The developed controller is different from the traditional adaptive impedance controller in a way that it does not need a predefined trajectory. Which is a big establishment as setting a set trajectory to a robot in assistive environment may not work since it has to interact with human and consciously react to certain changes. The controller made the robotic system to appear as a prescribed model. Thus the interaction behavior can be varied by changing the parameters of the prescribed model. The closed loop error dynamics do not contain the prescribed model parameters. This makes it easier for the human to control or close the outer loop and use adaptive robotic interfaces.

The second part contains the outer loop design. Human in the loop is considered and theories of model reference control [30] is used for all the mathematical derivations. The series model reference control structure [29] is used and the human instead of working based on the reference signal only works with error signal between the wanted

and actual outputs plus the reference signal. This can account for the fact that the human himself acts as a controller and reacts to the error of its action.

Even though the second part of the thesis gave good results, the control structure can be modified further to make it more realistic and acceptable and more task oriented. Different control structures can be used to complete the outer loop. An additional rule based outer loop can be added on top of the existing structure to achieve specific tasks or task based cost functions can be generated to perform a given task.

References

[1]. E. Gribovskaya, A. Kheddar, and A. Billard, “Motion learning and adaptive impedance control for robot control during physical interaction with humans,” Proc IEEE Int. Conf. Robotics and Automation, pp. 4326-4332, May 2011.

[2]. M. Kalakrishnan, L. Righetti, P. Pastor, and S. Schaal, “Learning force control policies for compliant motion,” Proc. IEEE Int. Conf. Intelligent Robots and Systems, pp. 4639-4644, Sept. 2011.

[3]. P. Pastor, M. Kalakrishnan,S. Chiita, E. Theodoru, and S. Schaal, “Skill learning and task outcome prediction for manipulation,” Proc IEEE Int. Conf. Robotics and Automation, pp. 3828-3834, May 2011.

[4]. S. Suzuki and K. Furuta, “Adaptive impedance control to enhance human skill on a haptic interface systems,” J. Control Science and Engineering, preprint, 2012.

[5]. S. Suzuki, K. Kurihara, K. Furuta, F. Harashima, and Y. Pan, “Variable dynamic assist control on haptic system for human adaptive mechatronics,” in *Proceedings of the 44th IEEE Conference on Decision and Control, and the European Control Conference (CDC-ECC ’05)*, pp. 4596–4601, Seville, Spain, December 2005.

[6]. N. Hogan, “Impedance control: An approach to manipulation: Part I-Theory, Part II-Implementation, Part III- Applications,” ASME J. Dynamic Syst., Measure. Contr., vol. 107, pp. 1-24, Mar. 1985.

[7]. C. H. An, C. G. Atkeson, and J. M. Hollerbach, Model Based Control of a Robot Manipulator. Cambridge, MA. MIT Press, 1988.

[8]. R. Volpe and P. Khosla, “Theoretical analysis and experimental verification of a manipulator/sensor/environment model for force control,” in Proc. IEEE Int. Con$ Systems, Man, and Cybernetics, Los Angeles, LA, Nov. 1990, pp. 784-790.

[9]. J. T. Wen and S. Murphy, “Stability analysis of position and force control for robot arms,” IEEE Trans. Automat. Contr., vol. 36, no. 3, pp. 365-371, Mar. 1991.

[10]. T. Yabuta, T. Yamada, T. Tsujimura, and H. Sakata, “Force control of servomechanism using adaptive control,” IEEE Trans. Robotics Automat., vol. 4, no. 2, pp. 223-228, Apr. 1988.

[11]. W. Lu and Q. Meng,, “Impedance control with adaptation for robotic manipulations,” IEEE Trans. Robotics Automat., vol. 7, no. 3, pp. 408-415, June 1991.

[12]. L. Huang, S.S. Ge, and T.H. Lee, “An adaptive impedance control scheme for constrained robots,” Int. J. Computers, Systems, and Signals, vol. 5, no. 2, pp. 17-26, 2004.

[13]. S. S. Ge, C. C. Hang, L. C. Woon and X. Q. Chen, “Impedance control of robot manipulators using adaptive neural networks,” International Journal of Intelligent Control and Systems, Vol.2, No.3, pp.433- 452, 1998.

[14]. C. Canudas de Wit, B. Siciliano and G. Bastin(Eds), Theory of Robot Control, Springer, 1996.

[15]. F. Lewis, S. Jagannathan, and A. Ye¸sildirek, Neural Network Control Of Robot Manipulators And Non-Linear Systems, ser. Taylor & Francis systems and control book series. Taylor & Francis, 1999.

[16]. Chenguang Yang, Zhijun Li; Jing Li, “Trajectory Planning and Optimized Adaptive Control for a Class of Wheeled Inverted Pendulum Vehicle Models,” Systems, Man, and Cybernetics Society”, Vol. 43, No.1, pp.24 – 36, 2012.

[17]. S. Nicosia, P. Tomei, “Model reference adaptive control algorithms for industrial robots”, Automatica, Vol. 20, No. 5, pp 635-644, 1984.

[18]. Myoungho Sunwoo, Ka C. Cheok, and N. J. Huang, “Model Reference Adaptive Control for Vehicle Active Suspension Systems,” IEEE Transactions on Industrial Electronics, Vol. 38, No. 3, pp 217-222.

[19]. Kuo-Kai Shyu, , Ming-Ji Yang, Yen-Mo Chen, and Yi-Fei Lin, “Model Reference Adaptive Control Design for a Shunt Active-Power-Filter System,” IEEE Transactions on Industrial Electronics, Vol. 55, No. 1, pp 97-106.

[20]. F. Lewis, D. Dawson, and C. Abdallah, Robot Manipulator Control: Theory and Practice, ser. Control Engineering. Marcel Dekker, 2004.

[21]. Schilling, R.J, Fundamentals of Robotics. Englewood Cliffs, NJ: Prentice Hall, 1991.

[22]. J. Slotine and W. Li, Applied nonlinear control. Prentice Hall, 1991.

[23] F. Lewis, S. Jagannathan, and A. Ye¸sildirek, Neural Network Control Of Robot Manipulators And Non-Linear Systems, ser. Taylor & Francis systems and control book series. Taylor & Francis, 1999.

[24] F. Lewis, K. Liu, and A. Yesildirek, “Neural net robot controller with guaranteed tracking performance,” Neural Networks, IEEE Transactions on, vol. 6, No. 3, pp. 703–715, 1995.

[25]. R. C.Miall, D. J.Weir, D. M. Wolpert, and J. F. Stein, “Is the cerebellum a smith predictor?” Journal of Motor Behavior, vol. 25, no. 3, pp. 203–216, 1993.

[26]. D. L. Kleinman, S. Baron, andW. H. Levison, “An optimal control model of human response part I: theory and validation,” Automatica, vol. 6, no. 3, pp. 357–369, 1970.

[27]. K. Furuta, Y. Kado, S. Shiratori, and S. Suzuki, “Assisting control for pendulum-like juggling in human adaptivemechatronics,” Journal of Systems and Control Engineering IMechE, Vol. 225, no. 6, pp. 709–720, 2011.

[28]. Karl Johan Astrom , Bjorn Wittenmark ," Adaptive Control," Dover publications, Inc. Mineola, New York, 2nd Edition, 1995.

[29]. J. van Amerongen ," MRAS: Model Reference Adaptive Systems," Journal A. Vol. 22, No. 4, 1981.

[30]. Karl Johan Astrom , Bjorn Wittenmark ," Adaptive Control," Dover publications, Inc. Mineola, New York, 2nd Edition, pp. 185-260,1995.

[31]. Ioannou, P.A., and P.V. Kokotovic,"Instability analysis and improvement of robustness of adaptive control," Automatica, Vol.20, no.5, pp.583-594, 1984..

Biographical Information

Shaikh Md Rubayiat Tousif is a graduate student at University of Texas at Arlington. He is expected to complete his Masters in Electrical Engineering degree in May 2014. During his time as a graduate student he severed as a graduate research/ teaching assistant. Before coming to UTA he was an Instructor in American International University-Bangladesh (AIUB) and worked there for nearly three years. He also did his Bachelor in Engineering from AIUB. He received Summa Cum Laude in his under graduate studies. He is interested in advanced control system and its application to different systems. His interests also spans in the areas of power system analysis and design.